Sea Surface Temperature algorithm refinement and validation though ship-based infrared spectroradiometry

Peter J Minnett

Meteorology and Physical Oceanography
Rosenstiel School of Marine and Atmospheric Science
University of Miami

UNIVERSITY OF MIAMI

What is SST?

- The infrared emission from the ocean originates from the uppermost <1mm of the ocean – the skin layer.
- The atmosphere is in contact with the top of the skin layer.
- Ocean-to-atmosphere heat flow through the skin layer is by molecular conduction: this causes, and results from, a temperature gradient through the skin layer.
- Conventional measurements of SST are from submerged thermometers – a “bulk” temperature.
- T_{depth} below the influence of diurnal heating is the “foundation” temperature.

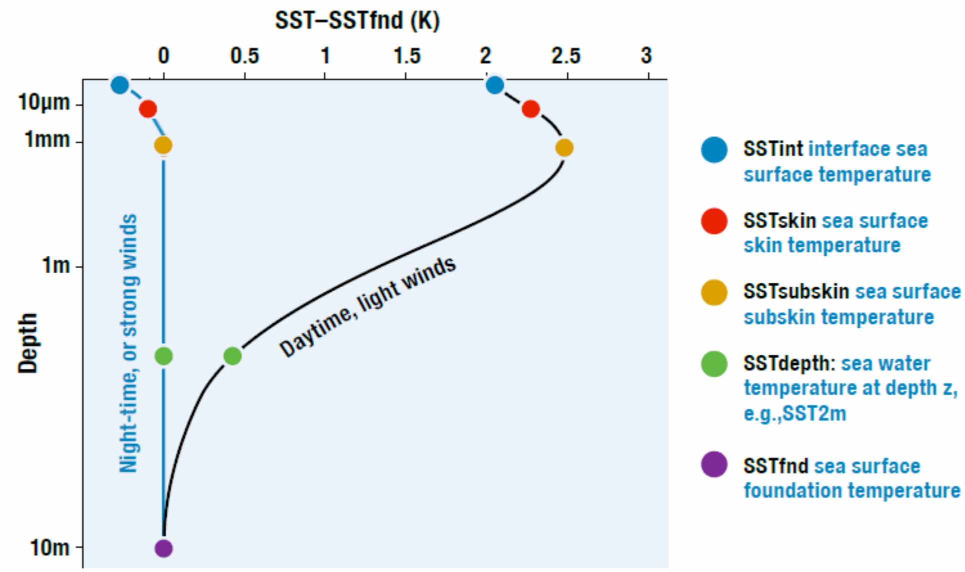

Figure 1: The hypothetical vertical profiles of temperature for the upper 10m of the ocean surface in high wind speed conditions or during the night (red) and for low wind speed during the day (black).

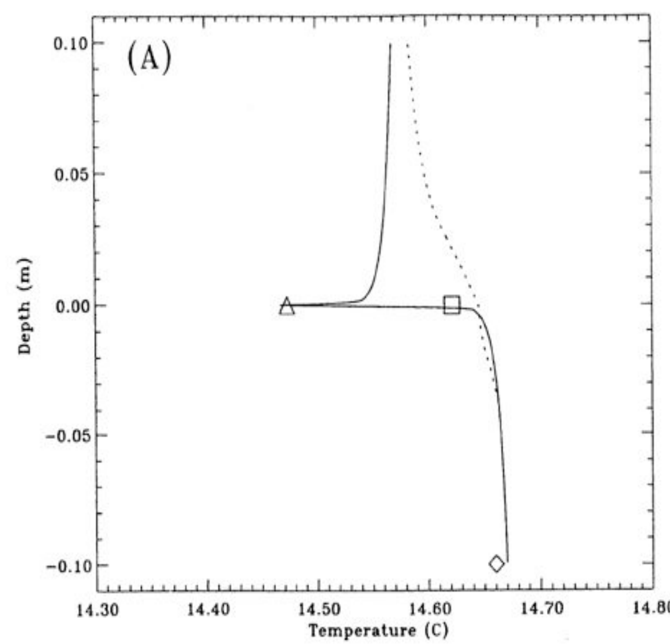

From Eifler, W. and C. J. Donlon, 2001: Modeling the thermal surface signature of breaking waves. J. Geophys. Res., 106, 27,163-27,185.

UNIVERSITY OF MIAMI

Marine-Atmospheric Emission Radiance Interferometer

The M-AERI is a Michelson-Morley Fourier-transform infrared (FTIR) interferometric spectroradiometer. These were first developed in the 1880's to make accurate measurements of the speed of light. Here we use it to make very accurate measurements of the sea-surface temperature, air temperature and profiles of atmospheric temperature and humidity. We also measure surface emissivity and the temperature profile through the skin layer, which is related to the flow of heat from the ocean to the atmosphere.

No. 203. Vol. XXXIV. NOVEMBER, 1887.

Established by BENJAMIN SILLIMAN in 1818.

THE

AMERICAN

JOURNAL OF SCIENCE.

EDITORS

JAMES D. AND EDWARD S. DANA.

ASSOCIATE EDITORS

PROFESSORS ASA GRAY, JOSIAH P. COOKE, AND JOHN TROWBRIDGE, OF CAMBRIDGE,

PROFESSORS H. A. NEWTON AND A. E. VERRILL, OF NEW HAVEN,

PROFESSOR GEORGE F. BARKER, OF PHILADELPHIA.

THIRD SERIES.

VOL. XXXIV.—[WHOLE NUMBER, CXXXIV.]

WITH PLATES II TO IX.

No. 203—NOVEMBER, 1887.

NEW HAVEN, CONN.: J. D. & E. S. DANA.
1887.

TUTTLE, MOREHOUSE & TAYLOR, PRINTERS, 371 STATE STREET.

Six dollars per year (postage prepaid). $6.40 to foreign subscribers of countries in the Postal Union. Remittances should be made either by money orders, registered letters, or bank checks.

THE

AMERICAN JOURNAL OF SCIENCE.

[THIRD SERIES.]

ART. XXXVI.—*On the Relative Motion of the Earth and the Luminiferous Ether*; by ALBERT A. MICHELSON and EDWARD W. MORLEY.*

THE discovery of the aberration of light was soon followed by an explanation according to the emission theory. The effect was attributed to a simple composition of the velocity of light with the velocity of the earth in its orbit. The difficulties in this apparently sufficient explanation were overlooked until after an explanation on the undulatory theory of light was proposed. This new explanation was at first almost as simple as the former. But it failed to account for the fact proved by experiment that the aberration was unchanged when observations were made with a telescope filled with water. For if the tangent of the angle of aberration is the ratio of the velocity of the earth to the velocity of light, then, since the latter velocity in water is three-fourths its velocity in a vacuum, the aberration observed with a water telescope should be four-thirds of its true value.†

* This research was carried out with the aid of the Bache Fund.

† It may be noticed that most writers admit the sufficiency of the explanation according to the emission theory of light; while in fact the difficulty is even greater than according to the undulatory theory. For on the emission theory the velocity of light must be greater in the water telescope, and therefore the angle of aberration should be less; hence, in order to reduce it to its true value, we must make the absurd hypothesis that the motion of the water in the telescope carries the ray of light in the opposite direction!

AM. JOUR. SCI.—THIRD SERIES, VOL. XXXIV, NO. 203.—NOV., 1887.

UNIVERSITY OF MIAMI

Michelson interferometer

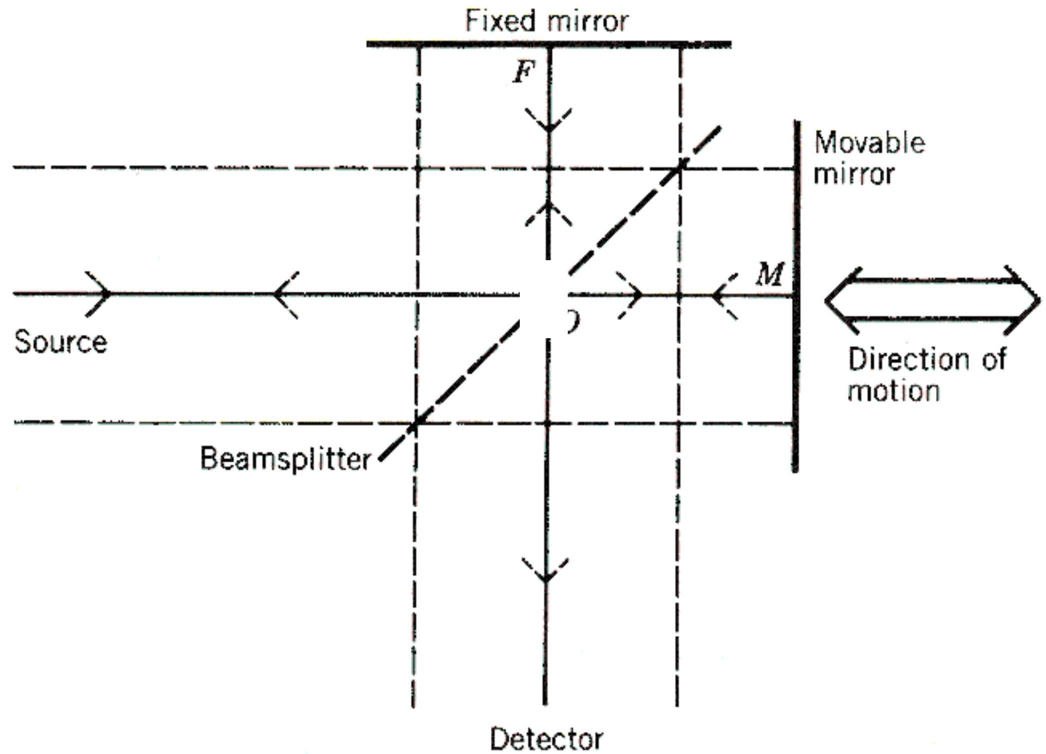

Schematic representation of a Michelson interferometer. The median ray is shown by the solid line, and the extremes of the collimated beam are shown by the broken lines.

The innards…..

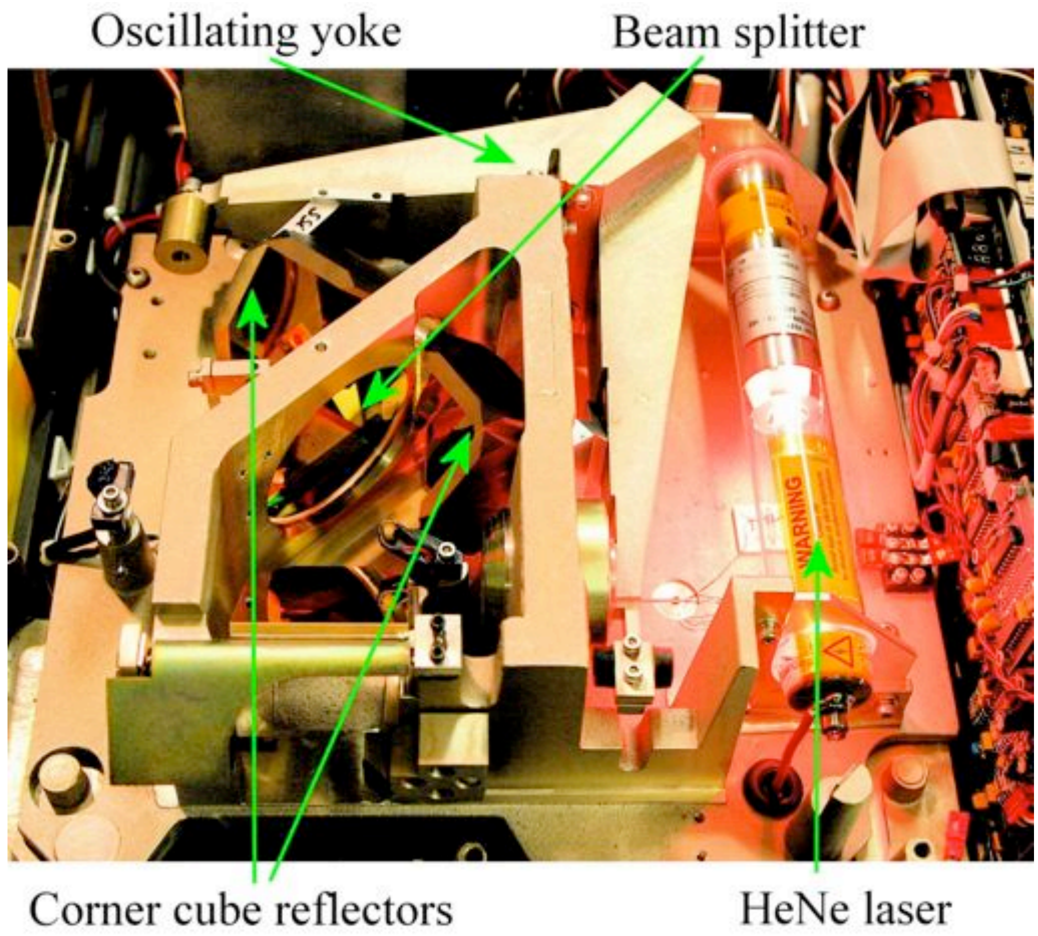

UNIVERSITY OF MIAMI

Marine - Atmospheric Emitted Radiance Interferometer. M-AERI

- Oscillating yoke provides a robust infrared radiometer for shipboard deployments.
- Visible laser used for wavelength calibration.
- Two blackbodies used for radiometric calibration.

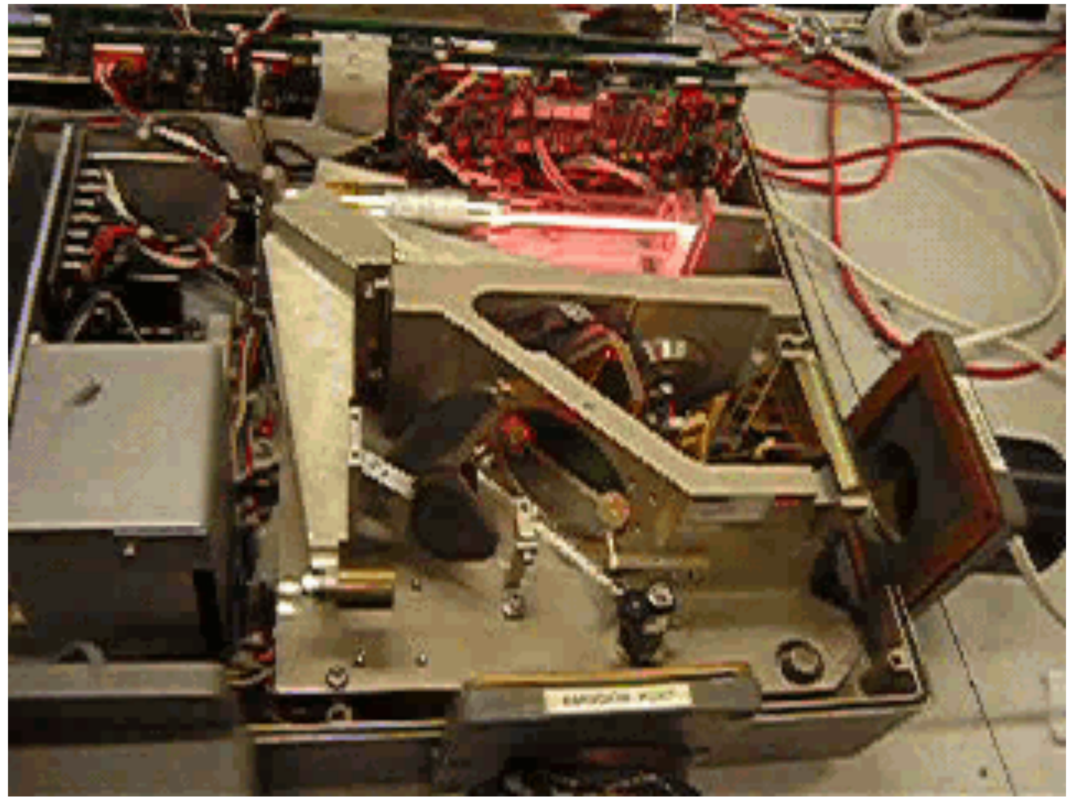

M-AERI cruises for MODIS, AATSR & AVHRR validation

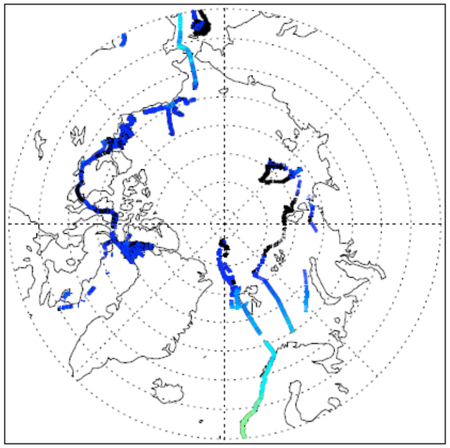

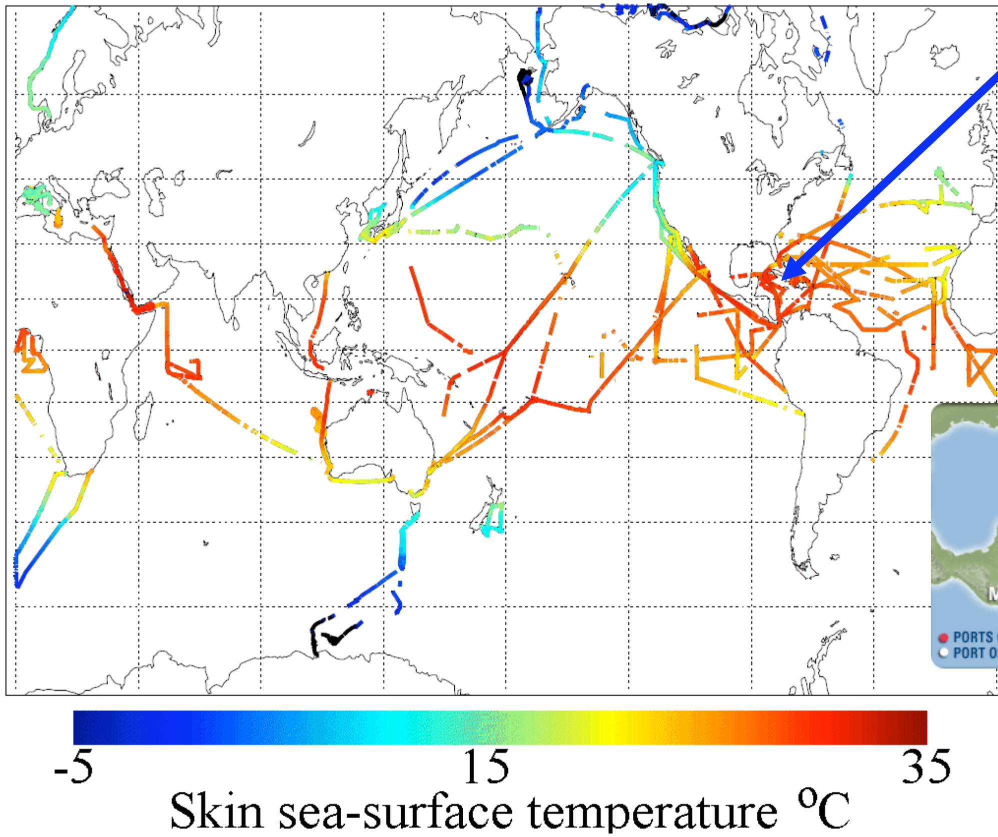

Explorer of the Seas

UNIVERSITY OF MIAMI

Explorer of the Seas: near continuous operation December 2000 – December 2007. Restarted February 2010.

ISAR cruises for MODIS, AATSR & AVHRR validation

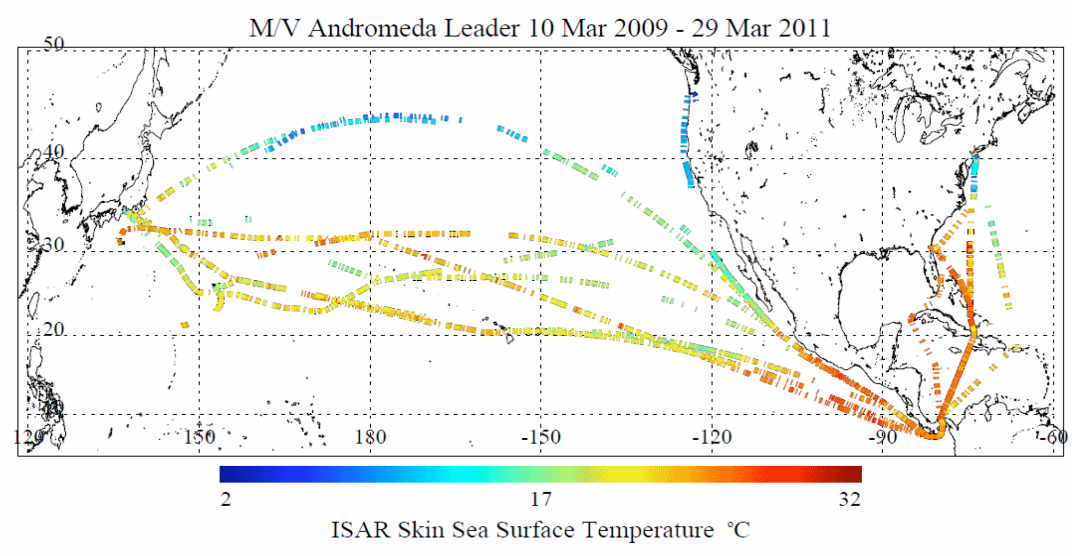

UNIVERSITY OF MIAMI

Measuring skin SST from ships

$$R_{\mathrm{water}}(\lambda, \theta) = \varepsilon(\lambda, \theta)B(\lambda, T_{\mathrm{skin}}) + (1 - \varepsilon(\lambda, \theta))R_{\mathrm{sky}}(\lambda, \theta) + R_h(\lambda, \theta)$$

$$T_{\mathrm{skin}} = B^{-1}\langle\{R_{\mathrm{water}}(\lambda, \theta) - [1 - \varepsilon(\lambda, \theta)]R_{\mathrm{sky}}(\lambda, \theta) - R_h(\lambda, \theta)\}/\varepsilon(\lambda, \theta)\rangle$$

- Scan-mirror mechanism for directing the field of view at complementary angles.
- Excellent calibration for ambient temperature radiances.
- Moderately good calibration at low radiances.

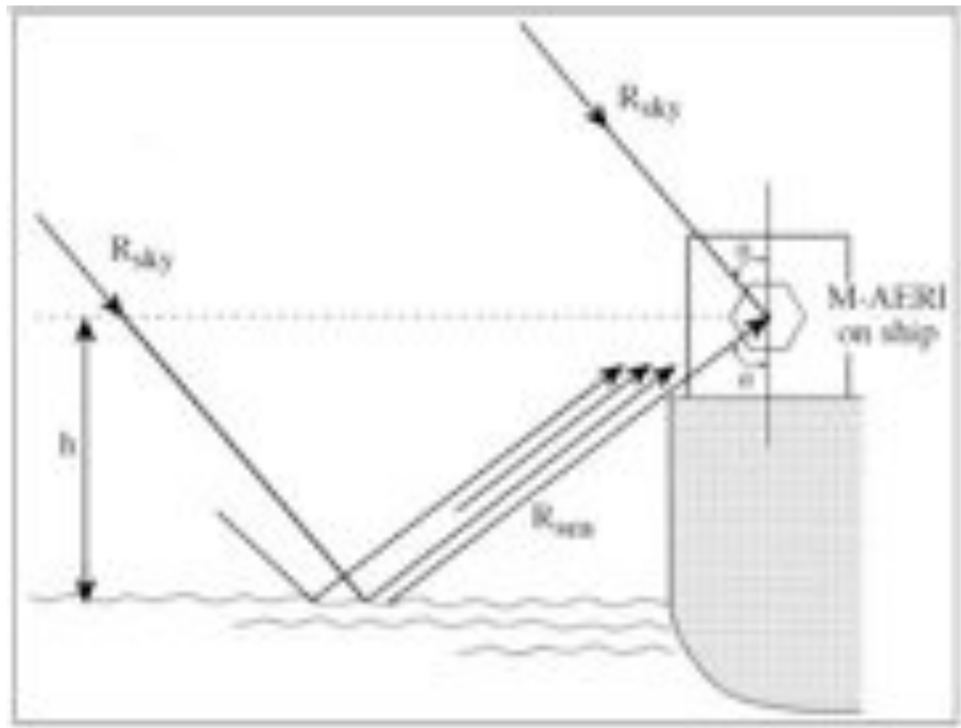

UNIVERSITY OF MIAMI

Sea surface emissivity (ε)

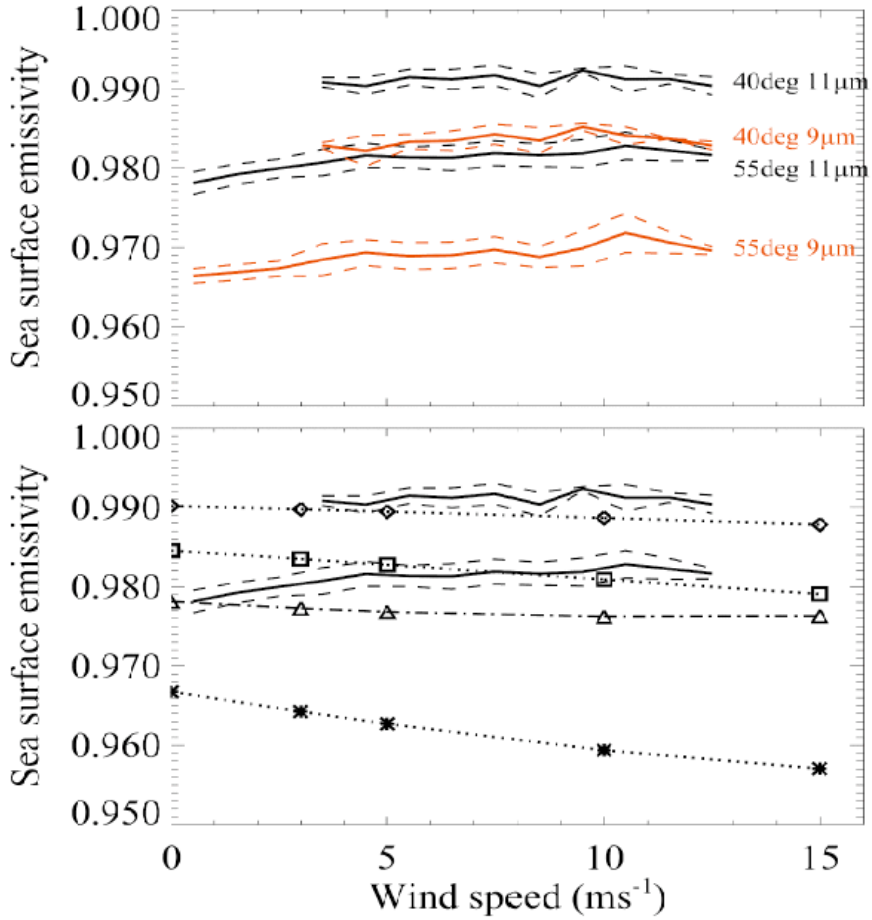

- Conventional wisdom gave decreasing ε with increasing wind.
- Not confirmed by at-sea hyperspectral measurements
- Improved modeling confirms at-sea measurements.

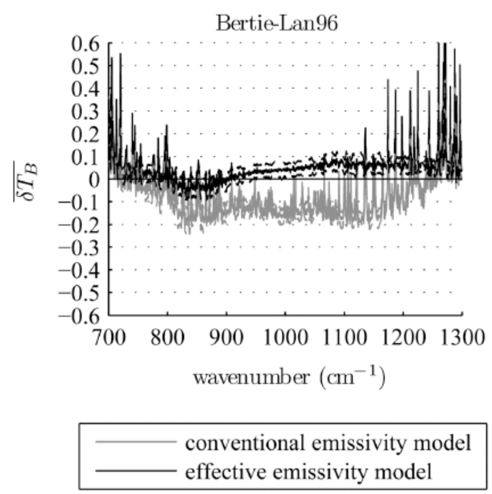

Hanafin, J. A. and P. J. Minnett, 2005: Infrared-emissivity measurements of a wind-roughened sea surface. *Applied Optics., **44, 398-411.***

Nalli, N. R., P. J. Minnett, and P. van Delst, 2008: Emissivity and reflection model for calculating unpolarized isotropic water surface-leaving radiance in the infrared. I: Theoretical development and calculations. *Applied Optics, **47, 3701-3721.***

Nalli, N. R., P. J. Minnett, E. Maddy, W. W. McMillan, and M. D. Goldberg, 2008: Emissivity and reflection model for calculating unpolarized isotropic water surface-leaving radiance in the infrared. 2: Validation using Fourier transform spectrometers. *Applied Optics, **47, 4649-4671.***

Internal Calibration

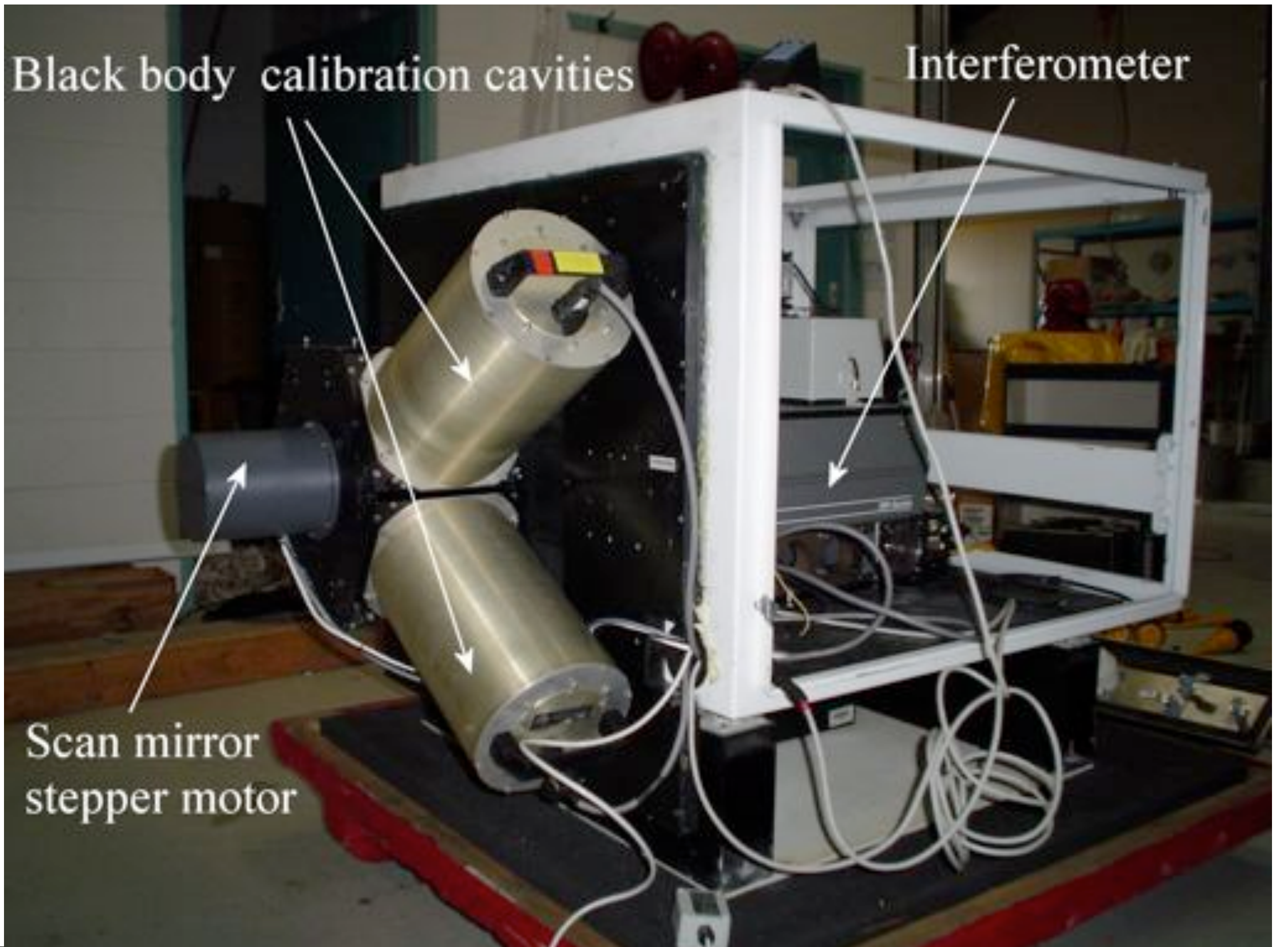

UNIVERSITY OF MIAMI

NIST water-bath black-body calibration target

See: Fowler, J. B., 1995. A third generation water bath based blackbody source, *J. Res. Natl. Inst. Stand. Technol.*, 100, 591-599

UNIVERSITY OF MIAMI

Traceability to NIST TXR

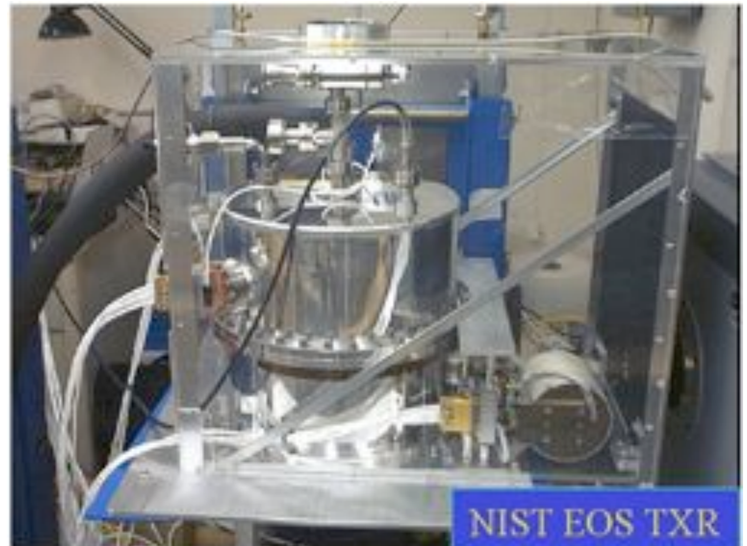

UNIVERSITY OF MIAMI

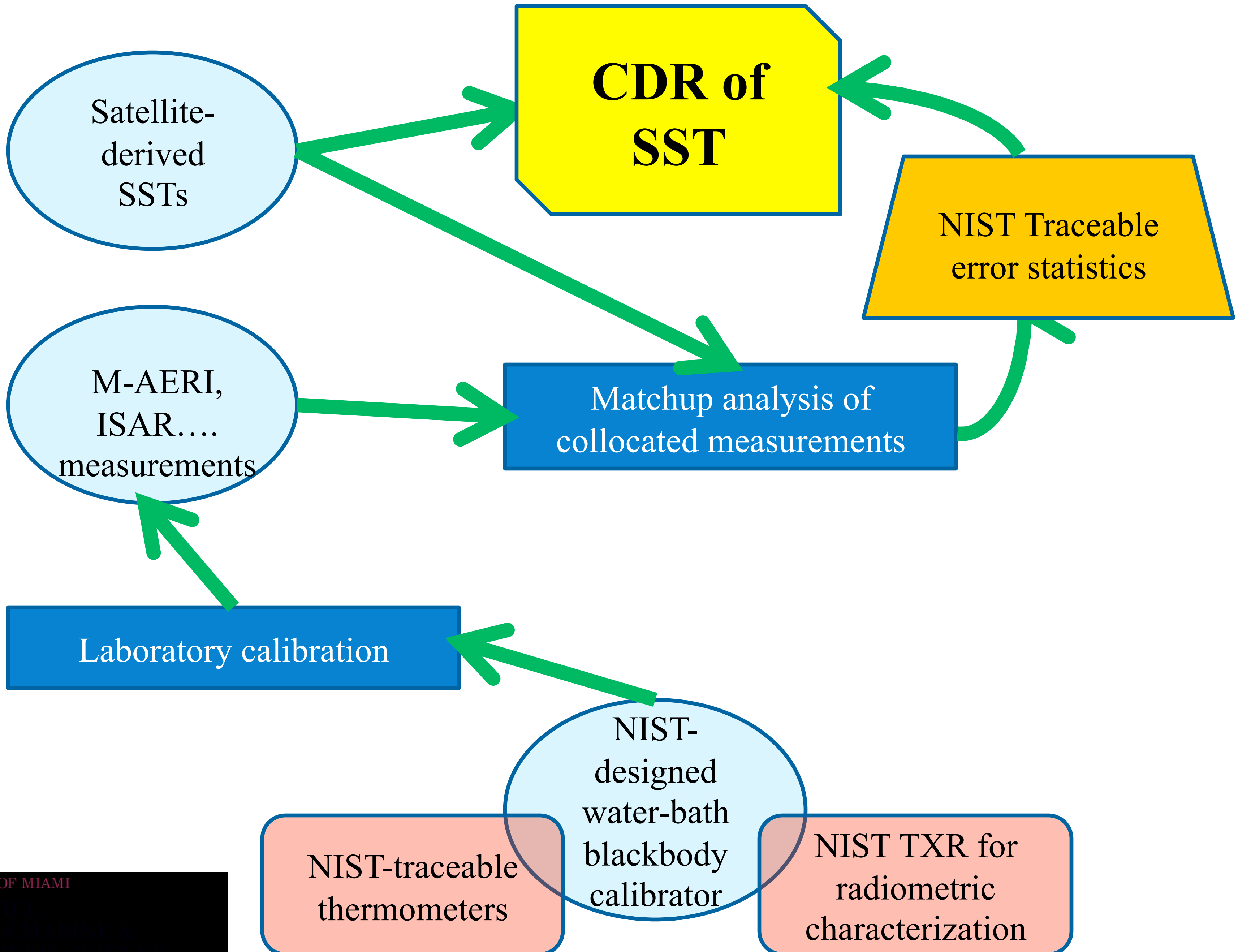

UNIVERSITY OF MIAMI

Next-generation ship-based FTIR spectroradiometer

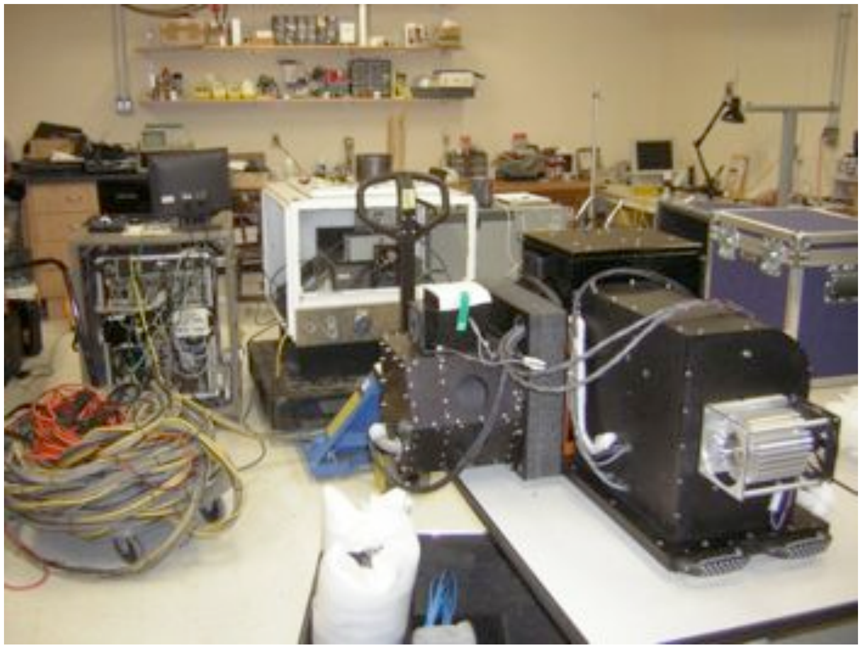

M-AERI Mk-2 undergoing tests at RSMAS.

Mk1 & Mk2

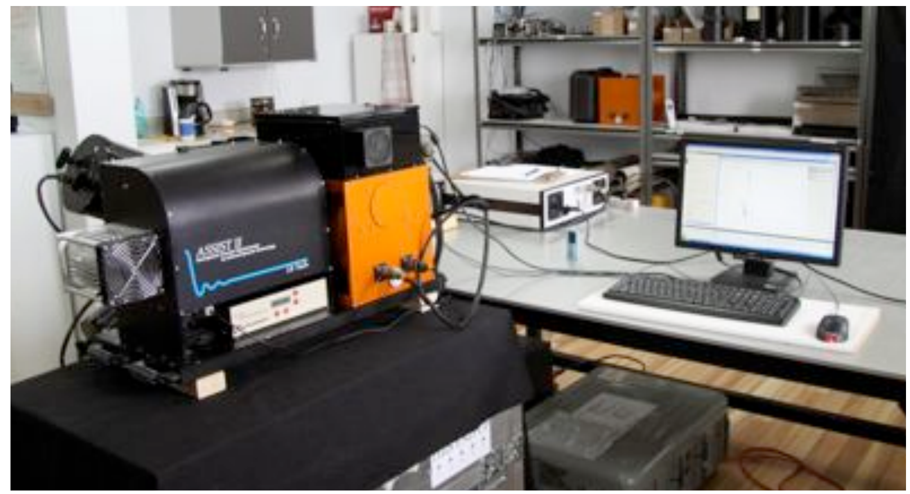

Sky emission measurements

Measurements taken in Quebec City, February 24, 2011.

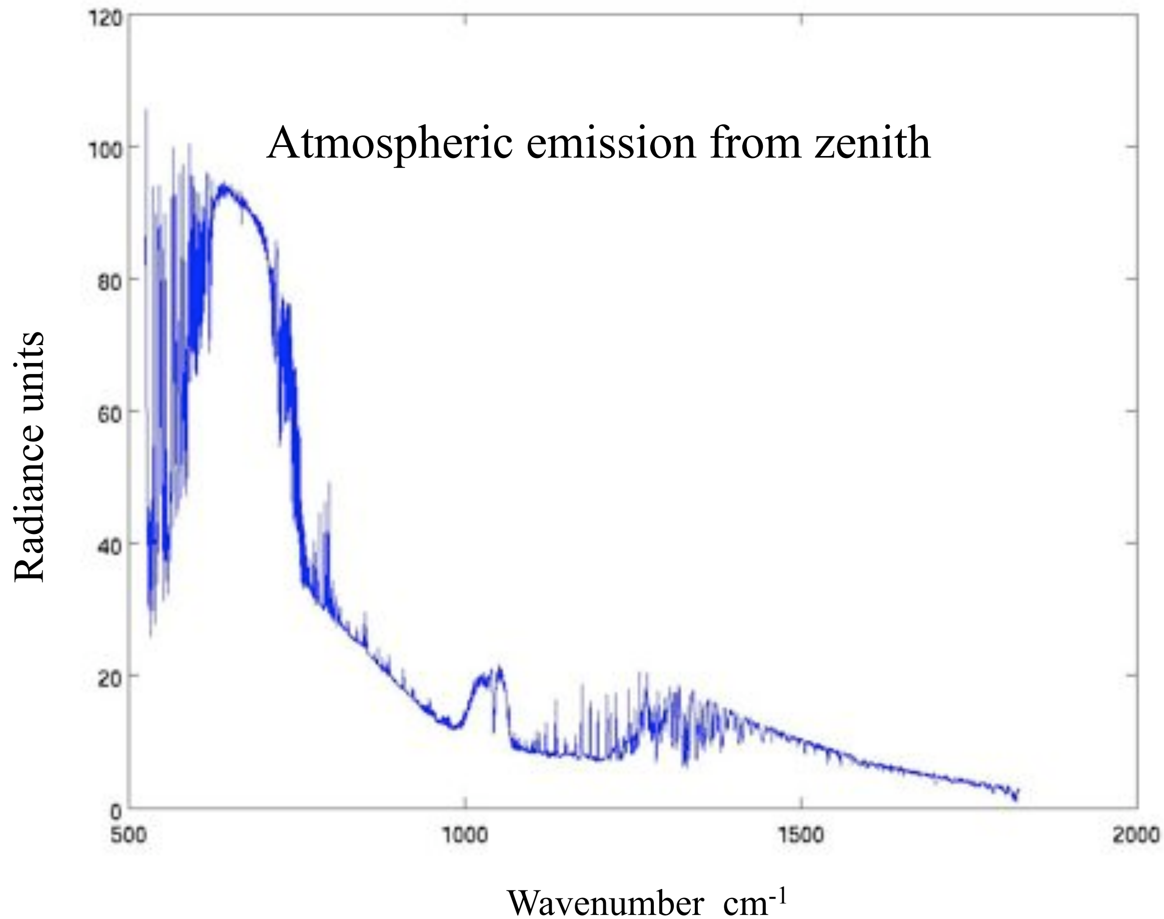

UNIVERSITY OF MIAMI

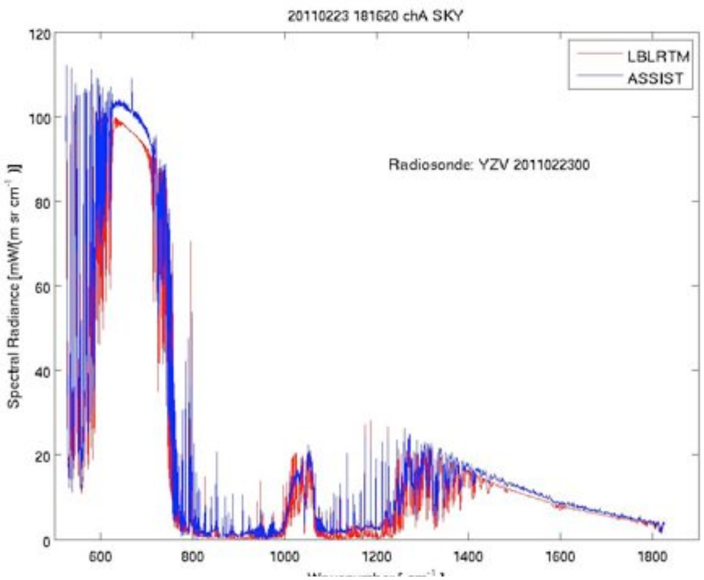
20110223 181620 chA SKY
LBLRTM
ASSIST
Radiosonde: YZV 2011022300
Spectral Radiance [mW/(m sr cm^{-1})]

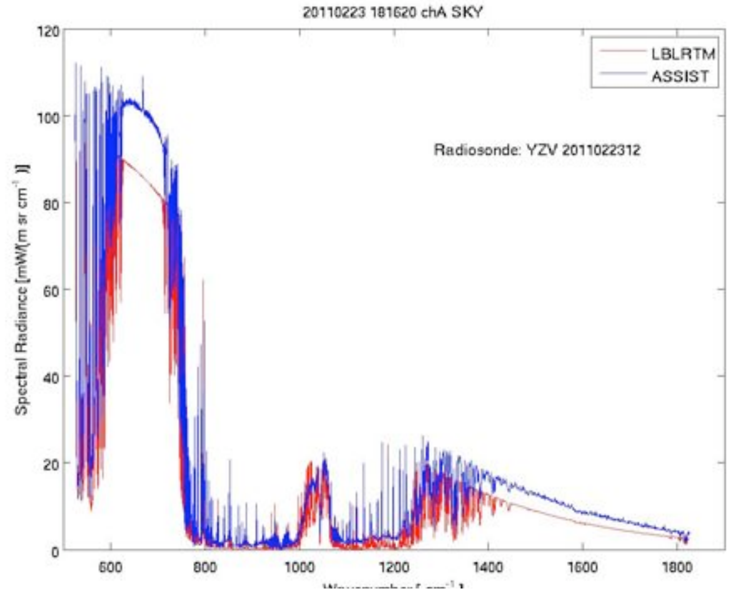
20110223 181620 chA SKY
LBLRTM
ASSIST
Radiosonde: YZV 2011022312
Spectral Radiance [mW/(m sr cm^{-1})]

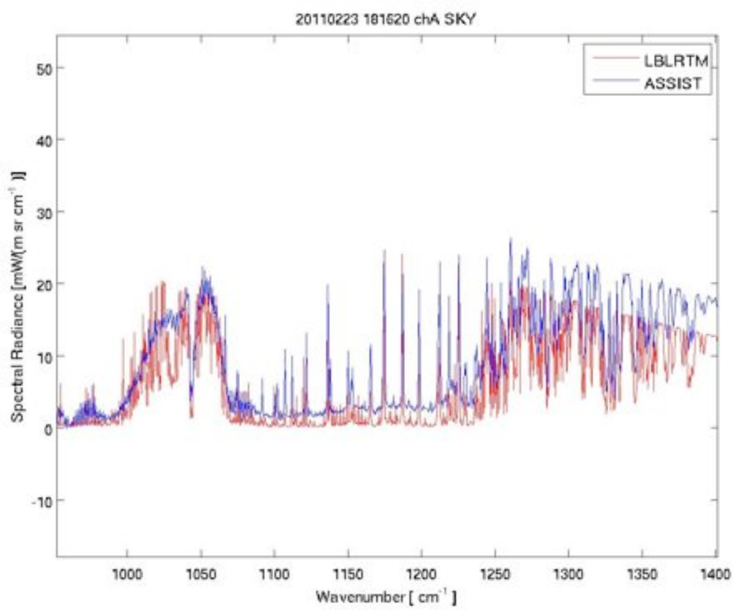
20110223 181620 chA SKY
LBLRTM
ASSIST
Spectral Radiance [mW/(m sr cm^{-1})]
Wavenumber [cm^{-1}]

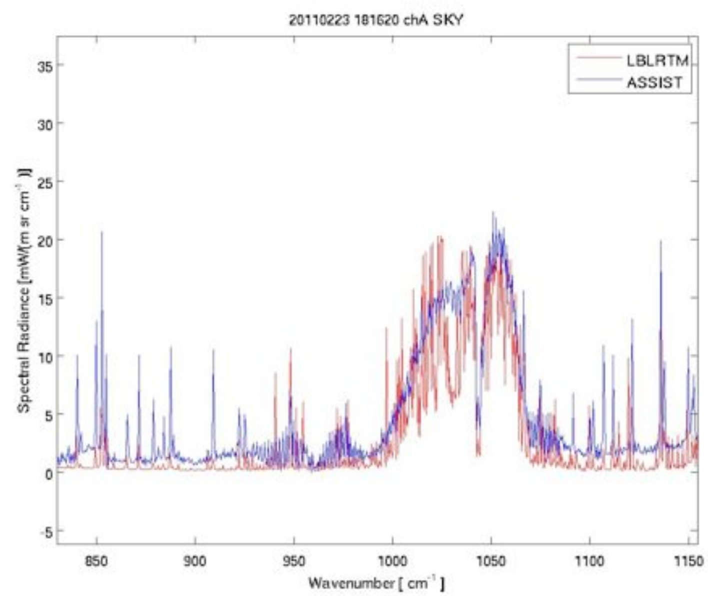
20110223 181620 chA SKY
LBLRTM
ASSIST
Spectral Radiance [mW/(m sr cm^{-1})]
Wavenumber [cm^{-1}]

Comparison with Arctic M-AERI measurements

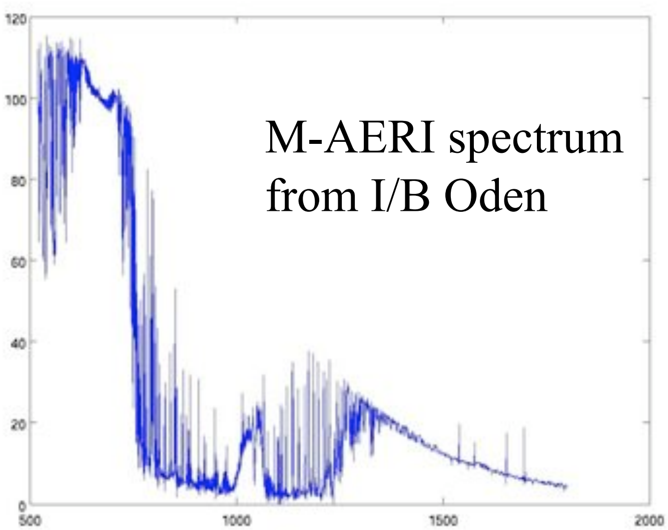

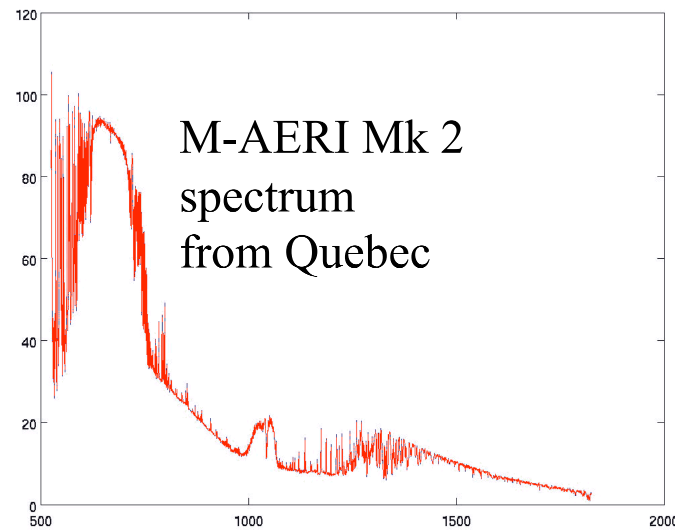

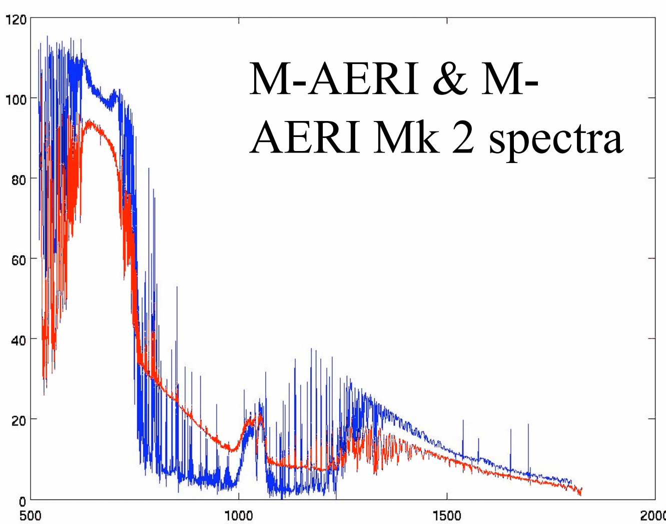

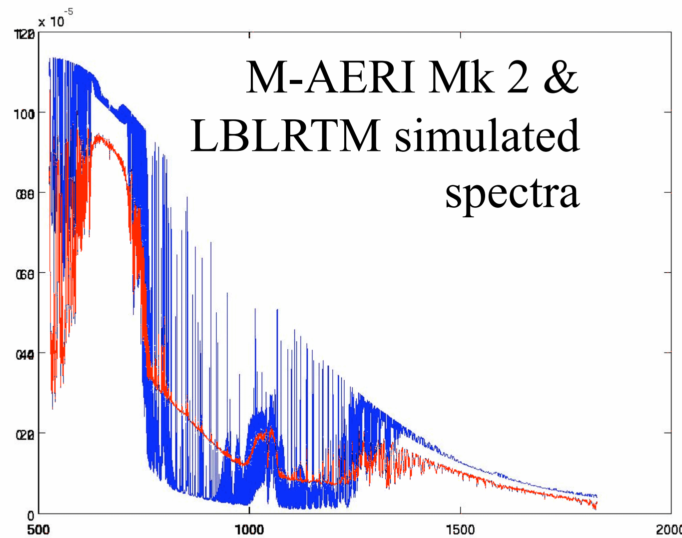

M-AERI Cruise opportunities

- Continue with *Explorer of the Seas*
- Two additional RCCL cruise liners
- NOAA Ship *Ronald H Brown* – Pirata moorings; July – August 2011
- R/V *Kilo Moana* – Samoa to Hawaii; November 2011
- Cunard *Queen Victoria*, Long Beach to Hawaii; February 2012 (tbc)
- VIIRS validation ???

UNIVERSITY OF MIAMI

Ron Brown cruise 2011

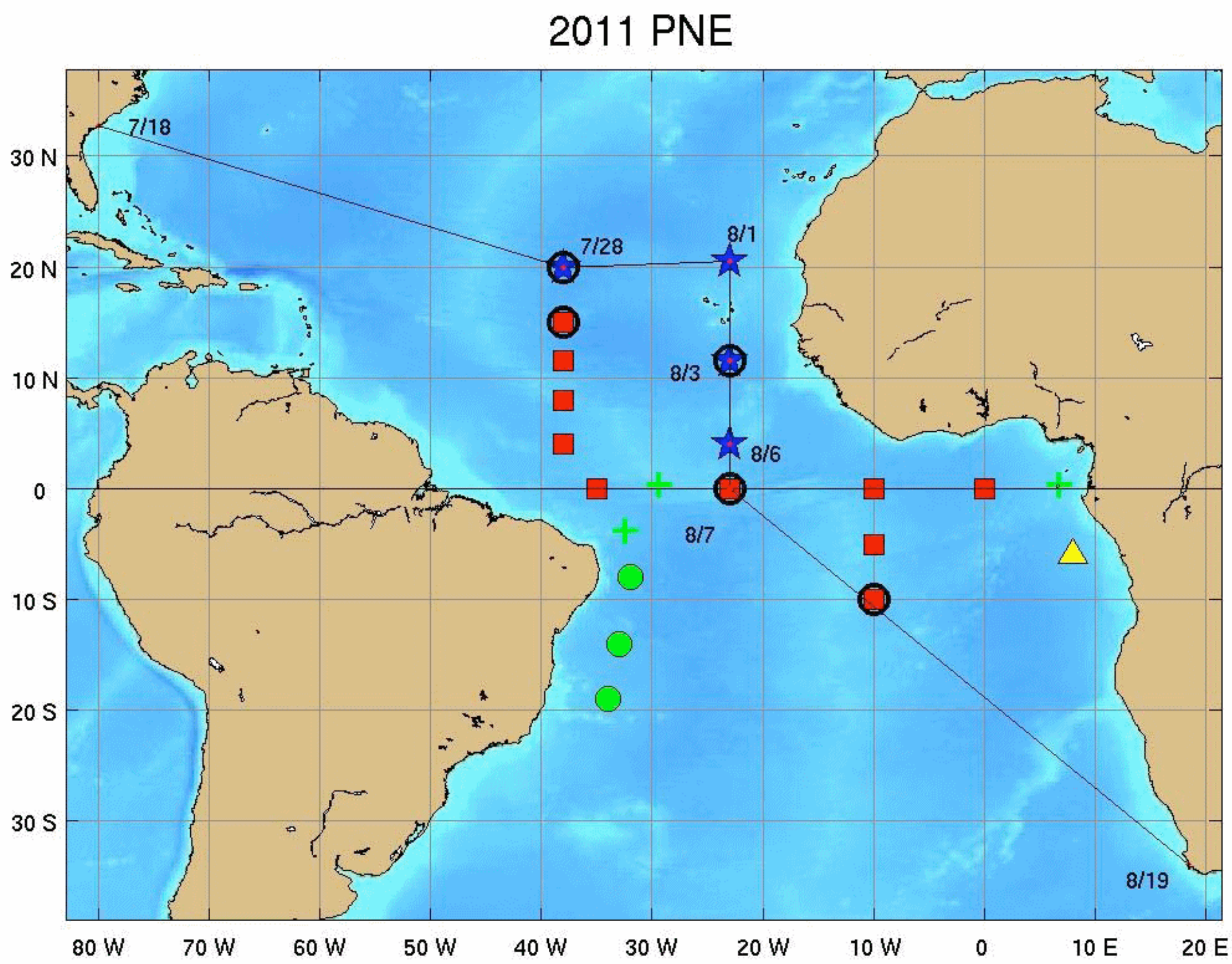

UNIVERSITY OF MIAMI

Equation Discovery using Genetic Algorithms

- Darwinian principles are applied to algorithms that "mutate" between successive generations
- The algorithms are applied to large data bases of related physical variables to find robust relationships between them. Only the "fittest" algorithms survive to influence the next generation of algorithms.
- Here we apply the technique to the MODIS matchup-data bases.
- The survival criterion is the size of the RMSE of the SST retrievals when compared to buoy data.

UNIVERSITY OF MIAMI

Successive generations of algorithms

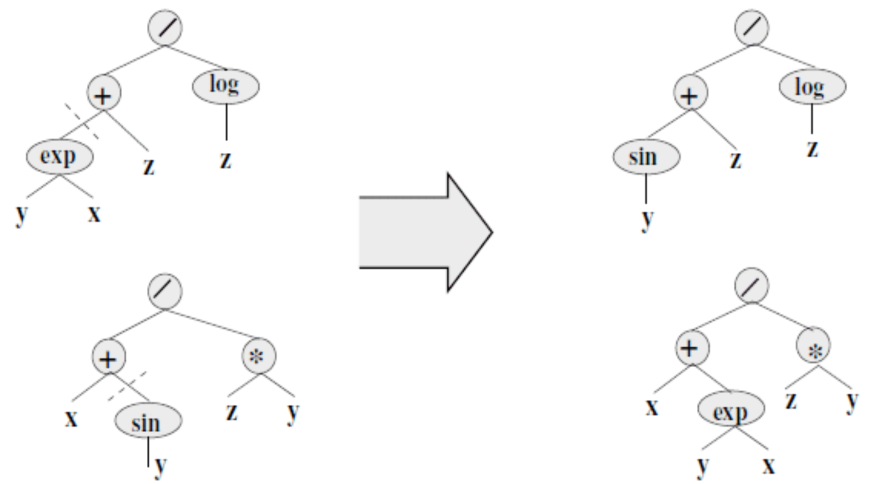

The formulae are represented by tree structures; the "recombination" operator exchanges random subtrees in the parents. Here the parent formulae $(y^x+z)/\log(z)$ and $(x+\sin(y))/zy$ give rise to children formulae $(\sin(y)+z)/\log(z)$ and $(x+y^x)/zy$. The affected subtrees are indicated by dashed lines.

Subsets of the data set can be defined in any of the available parameter spaces.

UNIVERSITY OF MIAMI

(From Wickramaratna, K., M. Kubat, and P. Minnett, 2008: Discovering numeric laws, a case study: CO_2 fugacity in the ocean. *Intelligent Data Analysis,* ***12,*** 379-391.)

Fittest Algorithm

The “fittest” algorithm takes the form:

$$SST = c_0 + c_1 T_{11} + c_2 (T_{11} - T_{12}) T_4 + \frac{c_3 (T_{11} - T_{12})}{\cos(1.13 \times \theta_s)} + c_4 \times \cos(1.0078 \times \theta_a - 0.7099)$$

where:

T_i is the brightness temperature at λ= i μm

θ_s is the satellite zenith angle

θ_a is the angle on the mirror (a feature of the MODIS paddle-wheel mirror design)

Which looks similar to the NLSST:

Non-Linear SST (NLSST)

$$NLSST = b_0 + b_1 * T_{11} + b_2 * T_{sfc} * (T_{11} - T_{12}) + b_3 * (T_{11} - T_{12}) * (\sec(\theta) - 1.)$$

UNIVERSITY OF MIAMI

Variants of the new algorithms

- Terra SST4:

$$SST = c_0 + c_1 T_{4.0} + c_2 (T_{3.9} - T_{4.0}) T_{3.9} + \frac{c_3 (T_{3.9} - T_{4.0})}{cos(1.13 \times \theta_s)} + c_4 \times cos(1.0078 \times \theta_a - 0.7099)$$

- Terra SSTnight, SSTday, SST:

$$SST = c_0 + c_1 T_{11} + c_2 (T_{11} - T_{12}) + \frac{c_3 (T_{11} - T_{12})}{cos(1.13 \times \theta_s)} + c_4 \times cos(1.0078 \times \theta_a - 0.7099)$$

- Terra newSSTnight:

$$SST = c_0 + c_1 T_{3.9} + c_2 (T_{3.9} - T_{4.0}) + \frac{c_3 (T_{3.9} - T_{4.0})}{cos(1.13 \times \theta_s)} + c_4 \times cos(1.0078 \times \theta_a - 0.7099)$$

- Aqua SST4:

$$SST = c_0 + c_1 T_{3.9} + c_2 (T_{3.9} - T_{4.0}) T_{3.9} + \frac{c_3 (T_{3.9} - T_{4.0})}{cos(1.13 \times \theta_s)} + c_4 \times cos(1.0078 \times \theta_a - 0.7099)$$

- Aqua SSTnight, SSTday, SST:

$$SST = c_0 + c_1 T_{11} + c_2 (T_{11} - T_{12}) + \frac{c_3 (T_{11} - T_{12})}{cos(1.13 \times \theta_s)} + c_4 \times cos(1.0078 \times \theta_a - 0.7099)$$

- Aqua newSSTnight:

$$SST = c_0 + c_1 T_{3.8} + c_2 (T_{11} - T_{12}) T_{3.9} + \frac{c_3 (T_{11} - T_{12})}{cos(1.13 \times \theta_s)} + c_4 \times cos(1.0078 \times \theta_a - 0.7099)$$

Coefficients are different for each equation

Note: No T_{sfc}

UNIVERSITY OF MIAMI

Mean SST retreival error. Aqua MODIS 11-12um SST. Day & Night. 1st Quarter 2007.

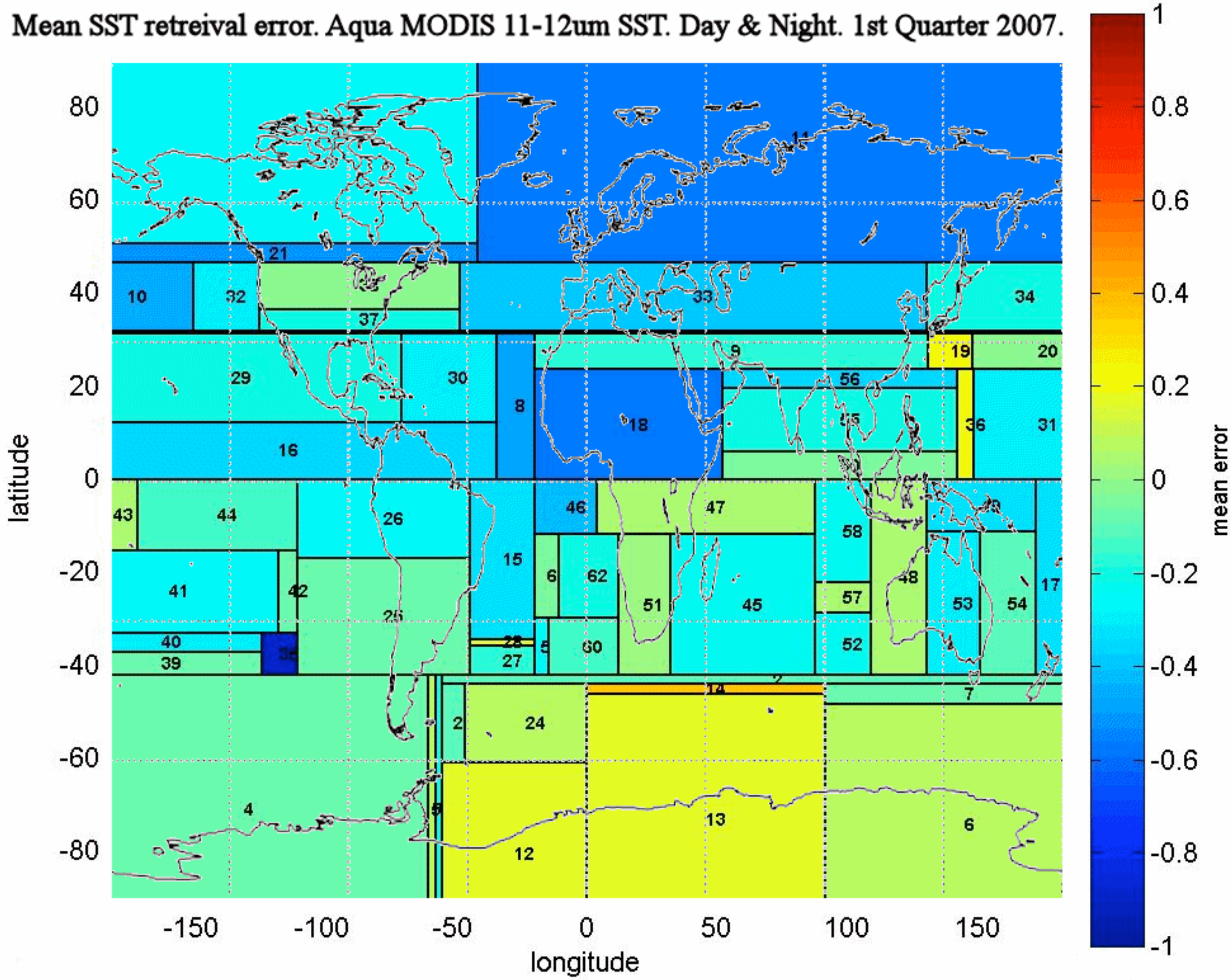

UNIVERSITY OF MIAMI

Std. Dev of SST retreival error. Aqua MODIS 11-12um SST. Day & Night. 1st Quarter 2007.

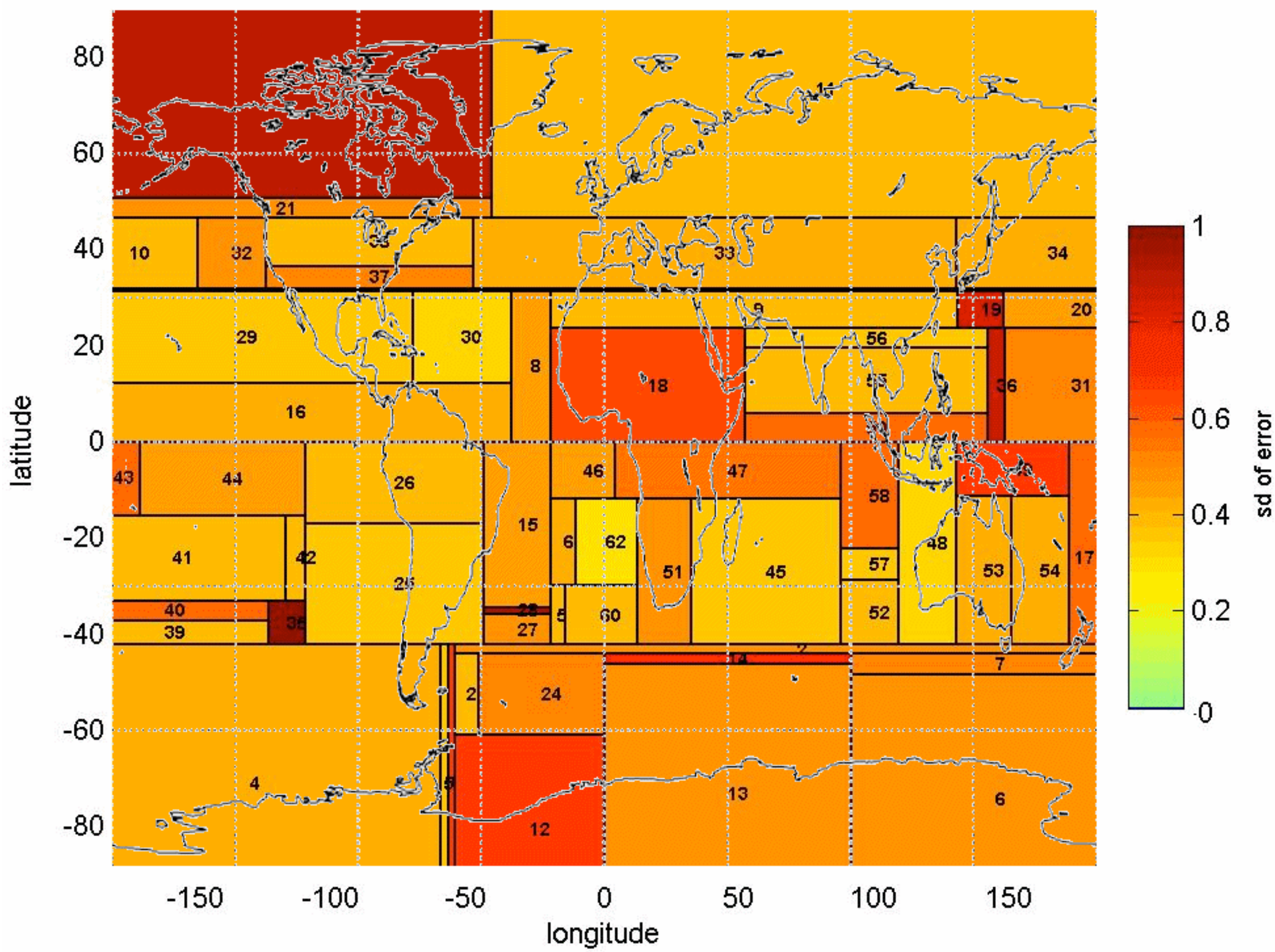

UNIVERSITY OF MIAMI

Preliminary Results

- The new algorithms with regions give smaller errors than NLSST or SST_4
- T_{sfc} term no longer required
- Night-time 4µm SSTs give smallest errors
- Aqua SSTs are more accurate than Terra SSTs
- Regression-tree induced in one year can be applied to other years without major increase in uncertainties
- SVM results do not out-perform GA+Regression Tree algorithms

Next steps

- Can some regions be merged without unacceptable increase in uncertainties?
- 180^{o}W should not necessarily always be a boundary of all adjacent regions.
- Iterate back to GA for regions – different formulations may be more appropriate in different regions.
- Allow scan-angle term to vary with different channel sets.
- Introduce “regions” that are not simply geographical.
- Suggestions?

UNIVERSITY OF MIAMI

Modeling Diurnal Warming and Cooling

- Prior models generally failed to raise temperatures sufficiently quickly, were not sufficiently responsive to changes in the wind speed, and retained too much heat into the evening and the night.
- New diurnal model that links the advantages of bulk models (speed) with the vertical resolution provided by turbulent closure models.
- Profiles of Surface Heating (POSH) model:

Surface forcing: (NWP or in situ)

+

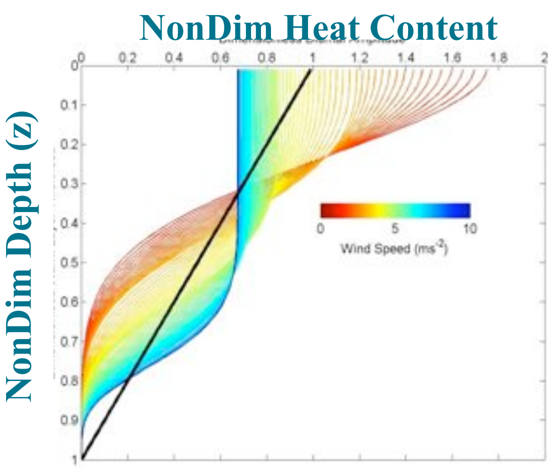

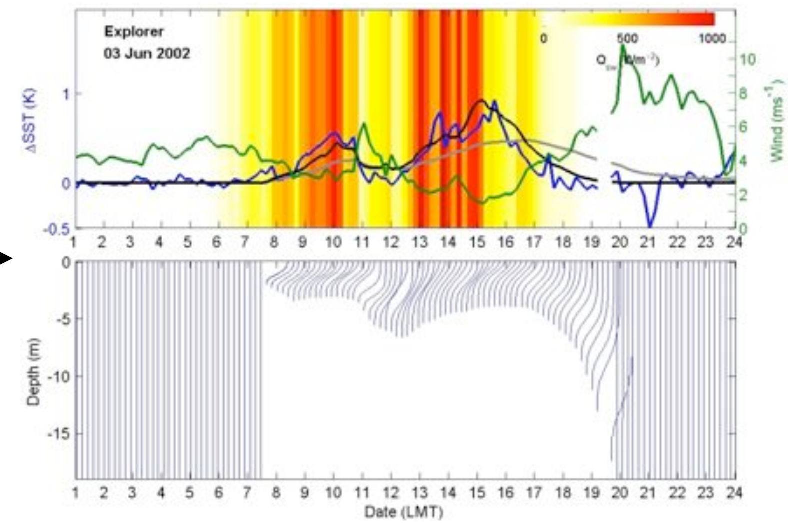

UNIVERSITY OF MIAMI

See Gentemann, C. L., P. J. Minnett, and B. Ward (2009). Profiles of Ocean Surface Heating (POSH): a new model of upper ocean diurnal thermal variability. Journal of Geophysical Research 114: C07017.

Diurnal Heating in Shallow Water (Xiaofang Zhu)

- How does the presence of the sea floor influence diurnal heating and cooling?
- Can a 1-D model be used in a hydro-dynamically complex situation to simulate the diurnal signals?
- Are satellite skin SSTs a good representation of the T_{depth} at the surface of coral reefs, for example?

NOAA's Integrated Coral Observing Network (ICON) Pylon

- Surface measurements include light (three band UV and PAR measurements), wind, air temperature, pressure, humidity and precipitation.
- Underwater measurements include light and temperature (CTD) measurements at nominal 1m and 3m depth
- Station water depths: about 6 meters
- Data resolution
- Nearby tidal station

UNIVERSITY OF MIAMI

http://ecoforecast.coral.noaa.gov/

Diurnal temperature signals

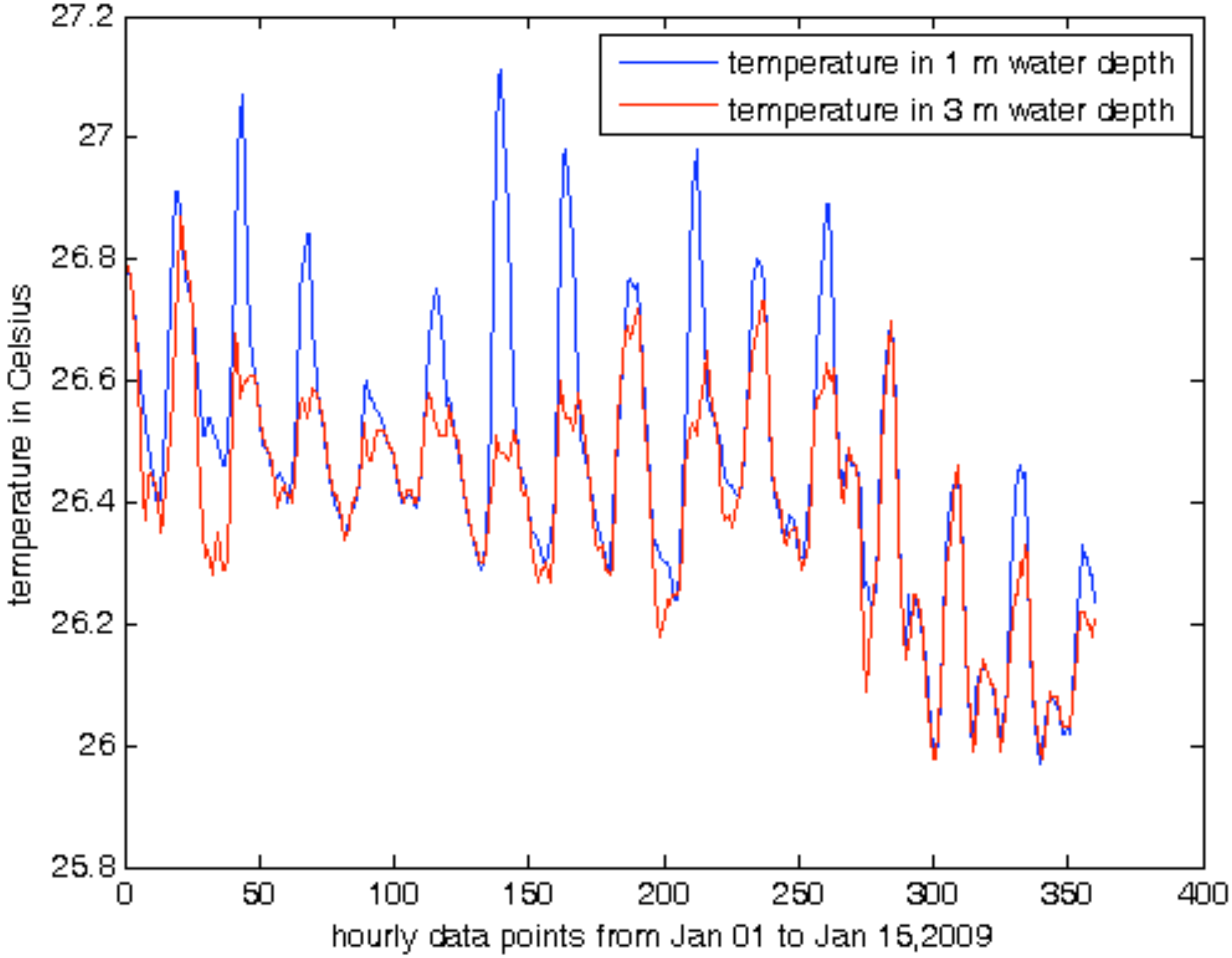

UNIVERSITY OF MIAMI

Little Cayman Coral Reef Temperatures

Internally recording thermometers added to the ICON pylon to resolve vertical temperature structure.

Significant differences are measured:

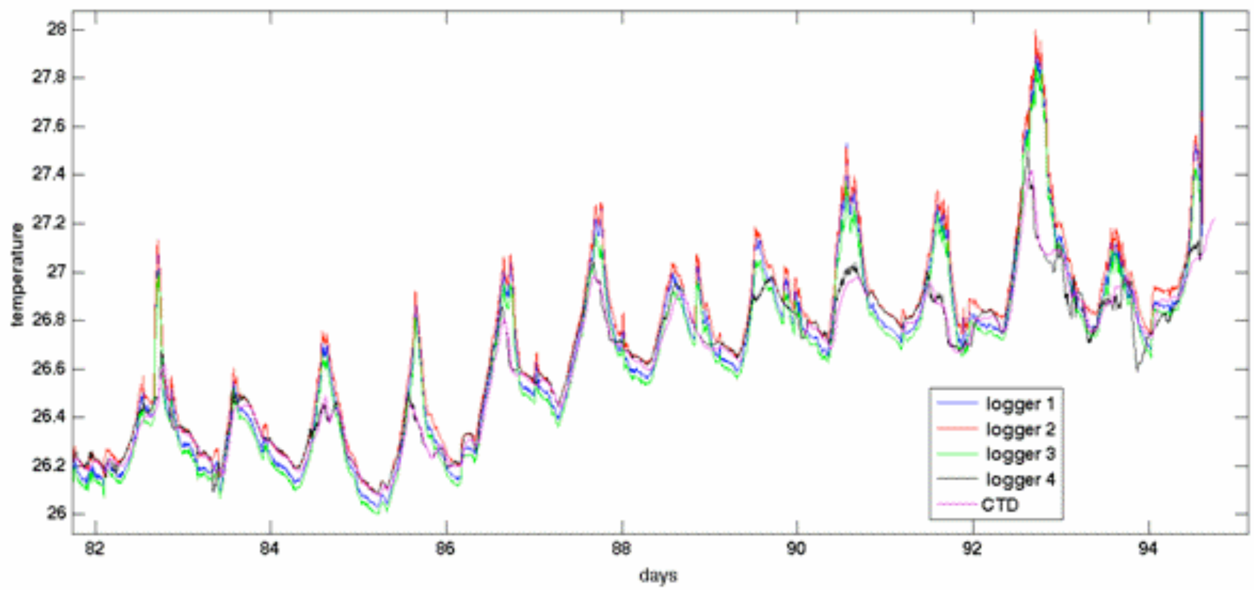

UNIVERSITY OF MIAMI

The Australian Great Barrier Reef.

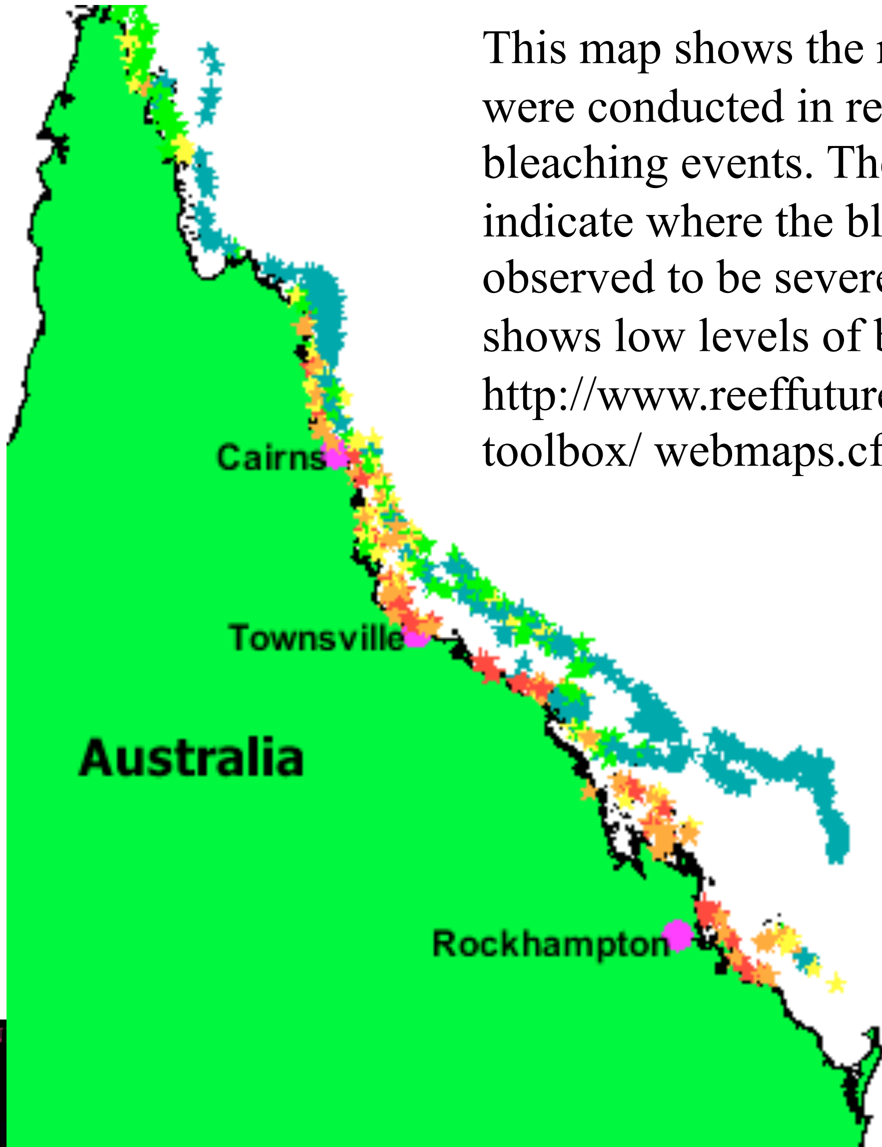

This map shows the reef surveys that were conducted in response to the bleaching events. The red colors indicate where the bleaching was observed to be severe while the green shows low levels of bleaching. From http://www.reeffutures.org/topics/toolbox/ webmaps.cfm#

Automatic weather stations will provide measurements of surface forcing for the model. E.g. at Davies Reef ~100km NE of Townsville, North Queensland. (http://www3.aims.gov.au/pages/facilities/weather-stations/weather-stations-images.html)

Temperature loggers on the GBR

- Data are obtained from in-situ data loggers deployed on the reef.
- Temperatures every 30 minutes and are exchanged and downloaded approximately every 12 months by divers.
- Temperature loggers on the reef-flat are generally placed just below Lowest Astronomical Tide level.
- Reef-slope (or where specified as Upper reef-slope) generally refers to depths 5 - 9 m while
- Deep reef-slope refers to depths of ~20 m.

UNIVERSITY OF MIAMI

Diurnal heating signal on the GBR

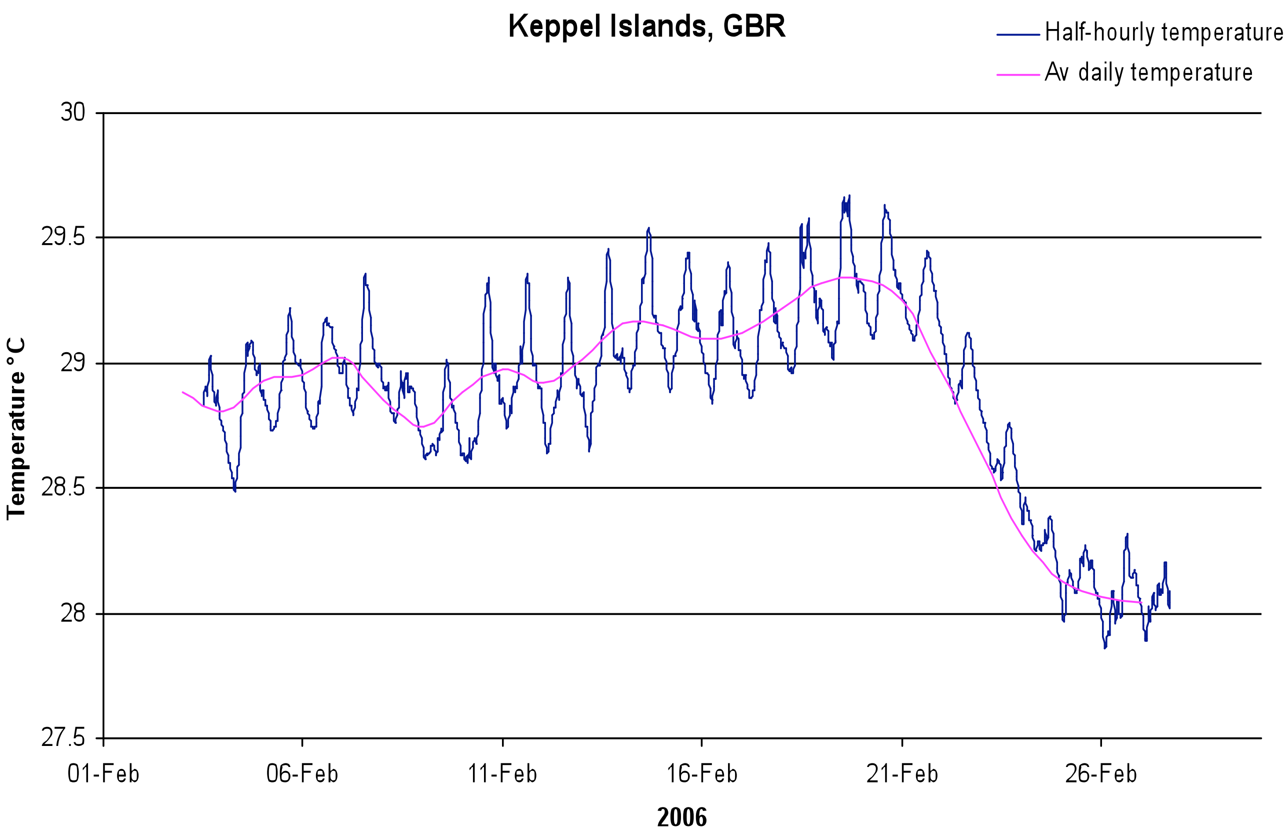

Example of the large diurnal heating during the 2006 bleaching event in the Keppel Islands (Great Barrier Reef). In situ temperatures were measured at 6m depth during the peak of the bleaching that killed 35% of coral in this area.

Future

- Continue MODIS (VIIRS?) validation cruises, including M-AERI Mk2
- Continue research into CDR generation
- Continue improving atmospheric correction algorithms
- Continue research into upper ocean thermal structure (skin effect, diurnal heating….)

UNIVERSITY OF MIAMI

Thank you for your attention.

Questions?

Aqua MODIS SST

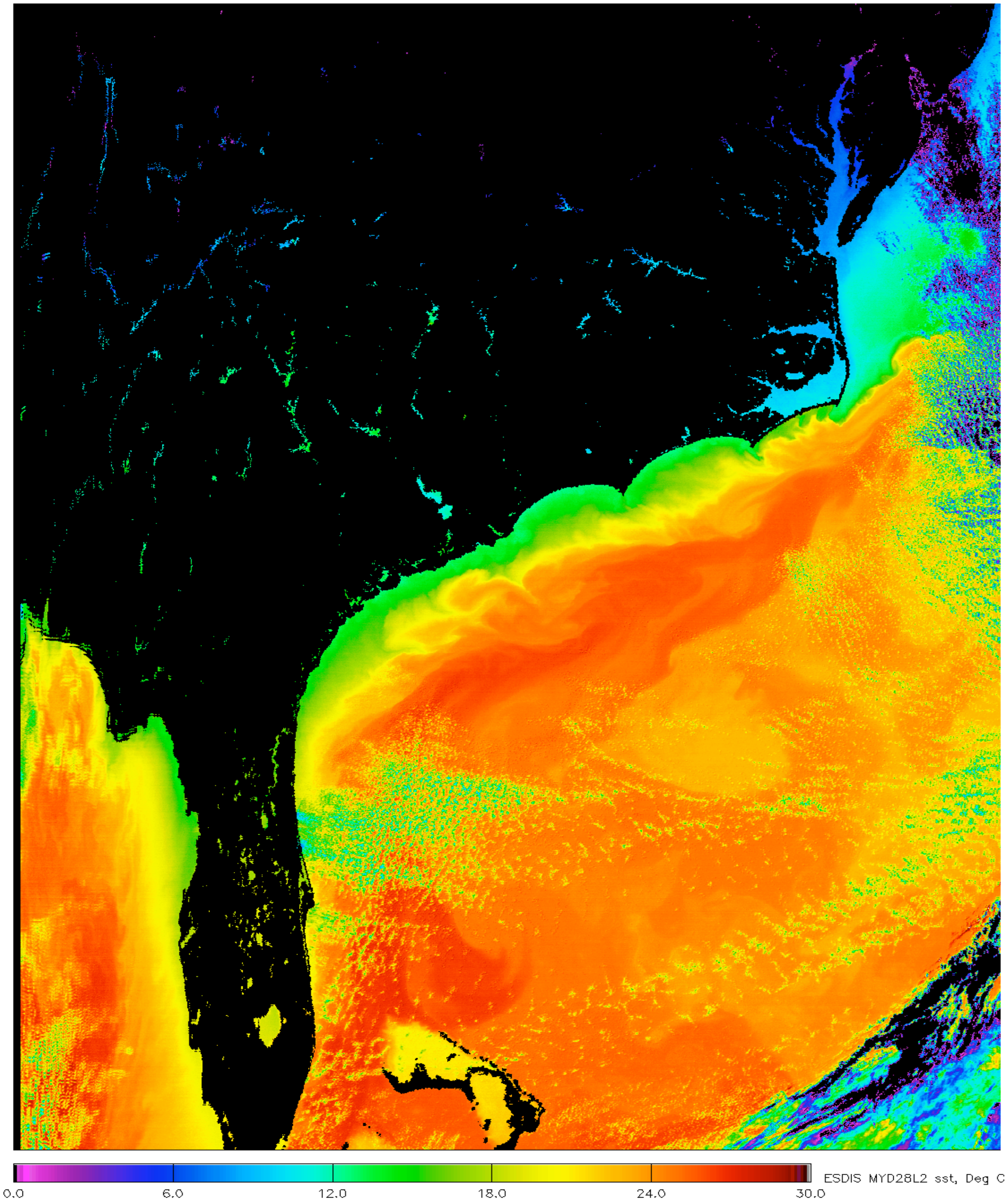

UNIVERSITY OF MIAMI

MODIS SST atmospheric correction algorithms

The form of the daytime and night-time algorithm for measurements in the long wave atmospheric window is:

$$SST = c_1 + c_2 * T_{11} + c_3 * (T_{11}-T_{12}) * T_{sfc} + c_4 * (\sec(\theta) - 1) * (T_{11}-T_{12})$$

where T_n are brightness temperatures measured in the channels at n μm wavelength, T_{sfc} is a 'climatological' estimate of the SST in the area, and θ is the satellite zenith angle. This is based on the Non-Linear SST algorithm.

[Walton, C. C., W. G. Pichel, J. F. Sapper and D. A. May (1998). "The development and operational application of nonlinear algorithms for the measurement of sea surface temperatures with the NOAA polar-orbiting environmental satellites." Journal of Geophysical Research **103** 27,999-28,012.]

The MODIS night-time algorithm, using two bands in the 4μm atmospheric window is:

$$SST4 = c_1 + c_2 * T_{3.9} + c_3 * (T_{3.9}-T_{4.0}) + c_4 * (\sec(\theta) - 1)$$

Note, the coefficients in each expression are different. They can be derived in three ways:

- empirically by regression against SST values derived from another validated satellite instrument
- empirically by regression against SST values derived surface measurements from ships and buoys
- [illegible] by numerical simulations of the infrared radiative transfer through the atmosphere.

Genetic Mutation of Equations

- The **<u>initial population</u>** of formulae is created by a generator of random algebraic expressions from a predefined set of variables and operators. For example, the following operators can be used: {+, -, /, ×, √, exp, cos, sin, log}. To the random formulae thus obtained, we can include "seeds" based on published formulae, such as those already in use.
- In the **<u>recombination</u>** step, the system randomly selects two parent formulae, chooses a random subtree in each of them, and swaps these subtrees.
- The **<u>mutation of variables</u>** introduces the opportunity to introduce different variables into the formula. In the tree that defines a formula, the variable in a randomly selected leaf is replaced with another variable.

GA-based equation discovery

initial state: randomly generated formulas plus manually created "seed" formulas

1. Randomly selected mating partners exchange genetic information by the recombination operator.
2. 20% randomly selected individuals are subjected to mutation of variables; 20% randomly selected individuals are subjected to mutation of operators; and all individuals are subjected to mutation of coefficients.
3. All individuals are subjected to mutation of inter-region borders.
4. The fitness of each individual (children as well as parents) is calculated as the formula's error on the training data. The top 50% are retained, and the remaining formulas are discarded.
5. Unless a termination criterion is satisfied, return to step 1.

MODIS scan mirror effects

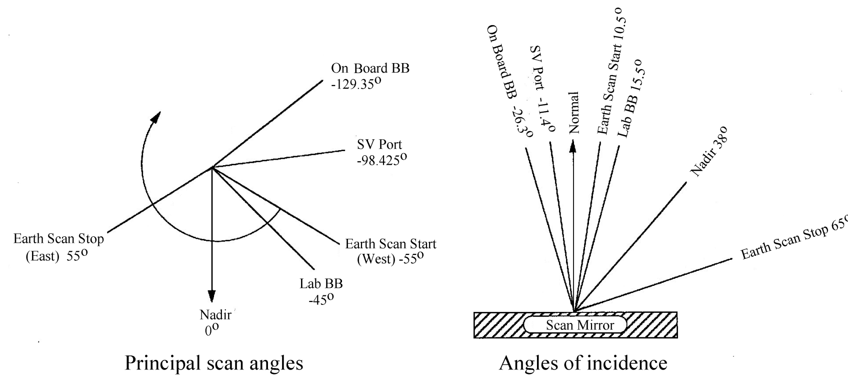

Mirror effects: two-sided paddle wheel has a multi-layer coating that renders the reflectivity in the infrared a function of wavelength, angle of incidence and mirror side.

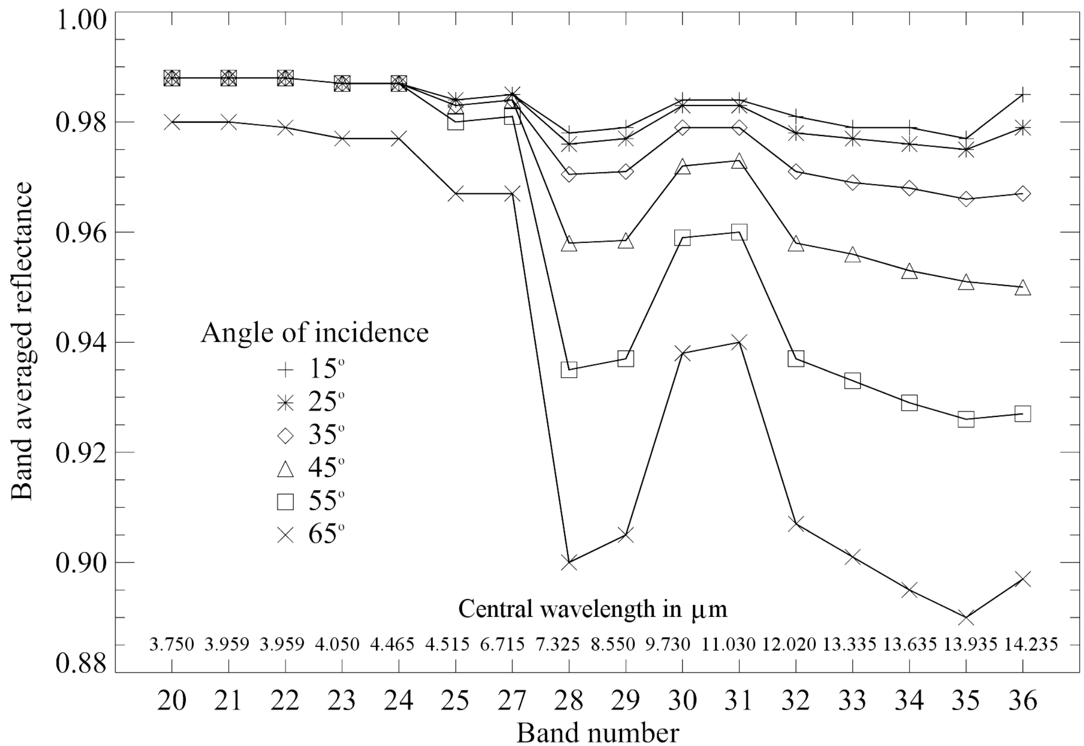

UNIVERSITY OF MIAMI

Regression tree

- Regions identified by the regression tree algorithm
- The tree is constructed using
  - input variables: latitude and longitude
  - output variable: *Error in retrieved SST*
- Algorithm recursively splits regions to minimize variance within them
- The obtained tree is pruned to the smallest tree within one standard error of the minimum-cost subtree, provided a declared minimum number of points is exceeded in each region
- Linear regression is applied separately to each resulting region (different coefficients result)

UNIVERSITY OF MIAMI

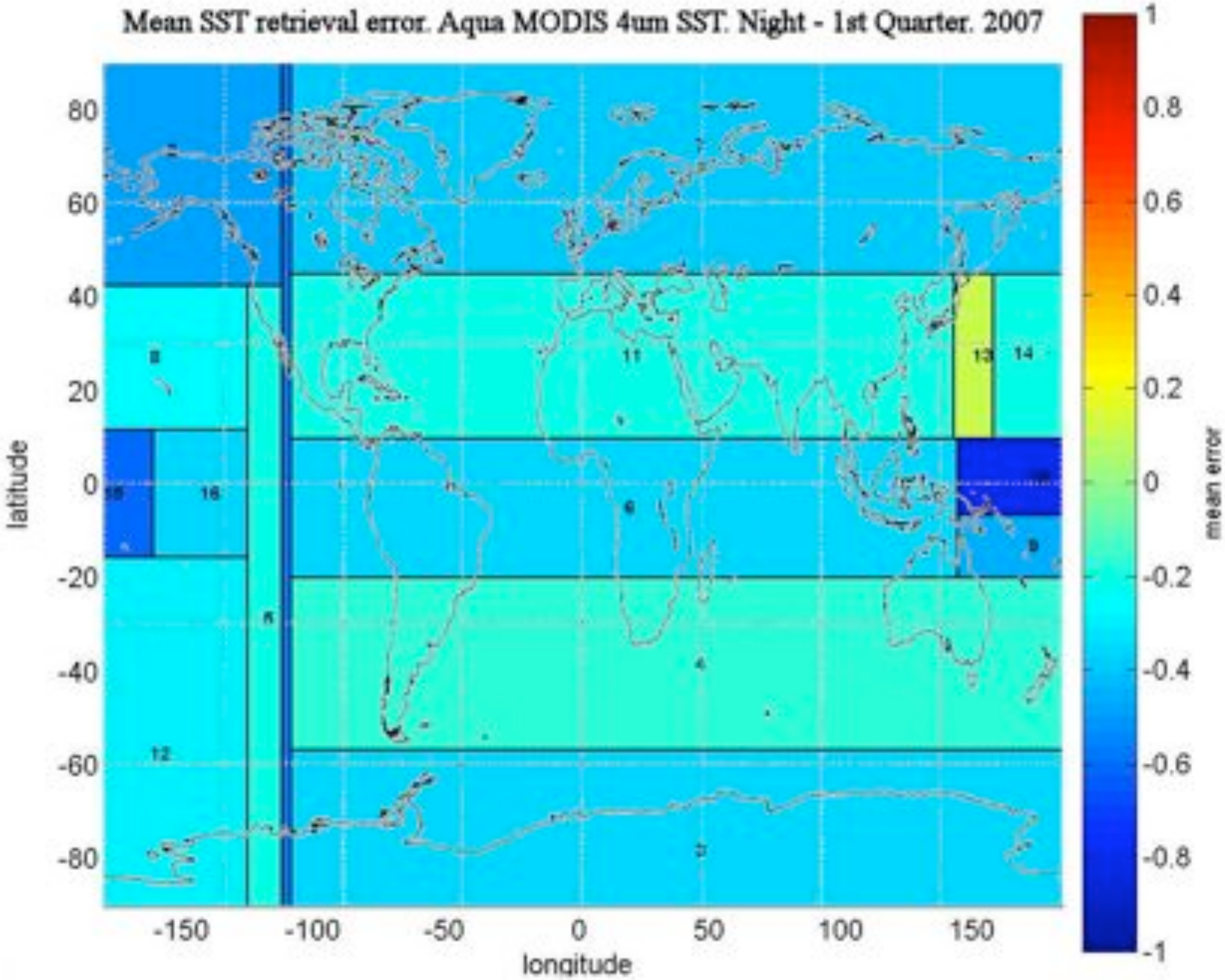

UNIVERSITY OF MIAMI

Std. Dev of SST retreival error. Aqua MODIS 4um SST. Night. 1st Quarter 2007.

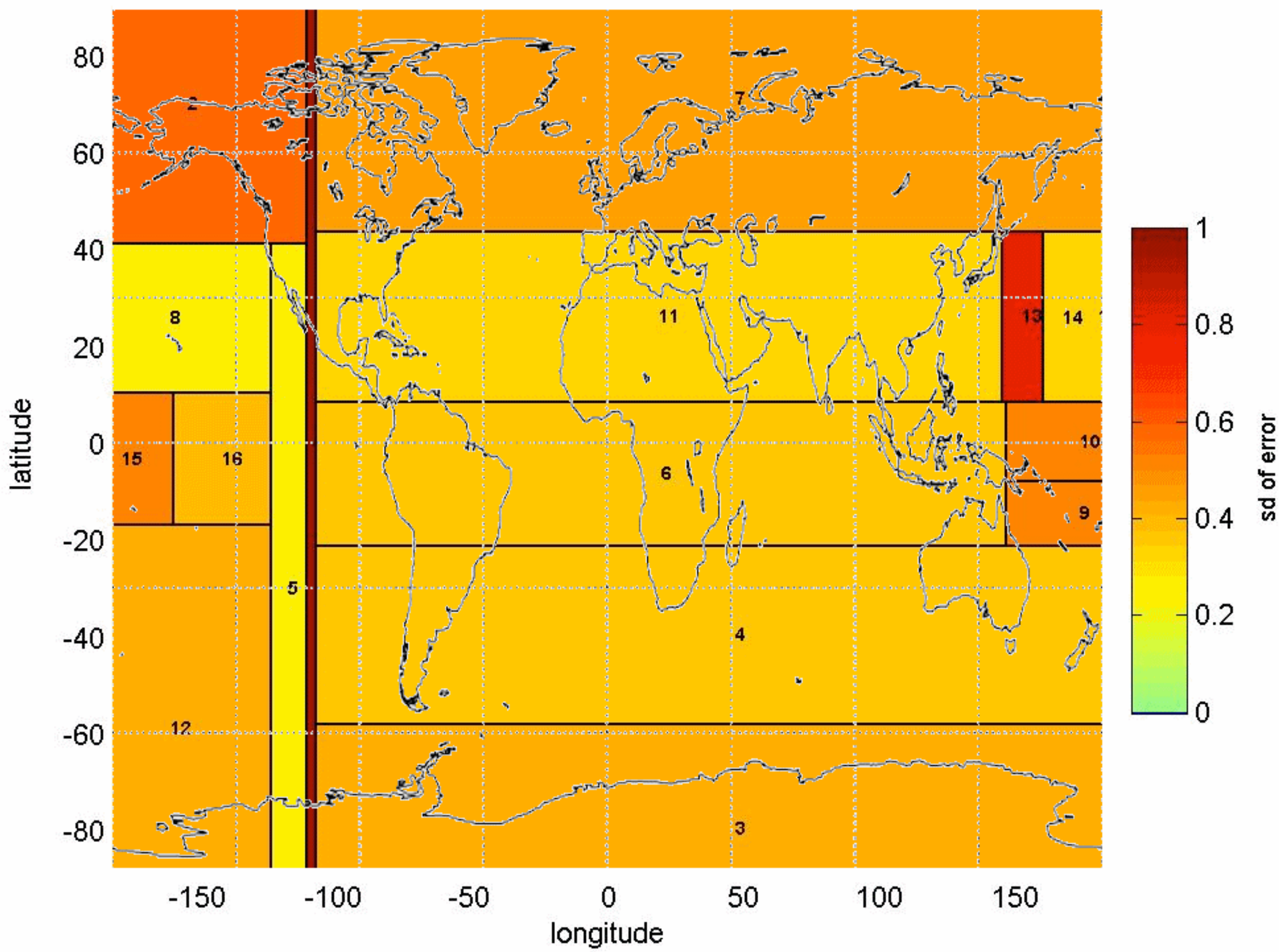

UNIVERSITY OF MIAMI

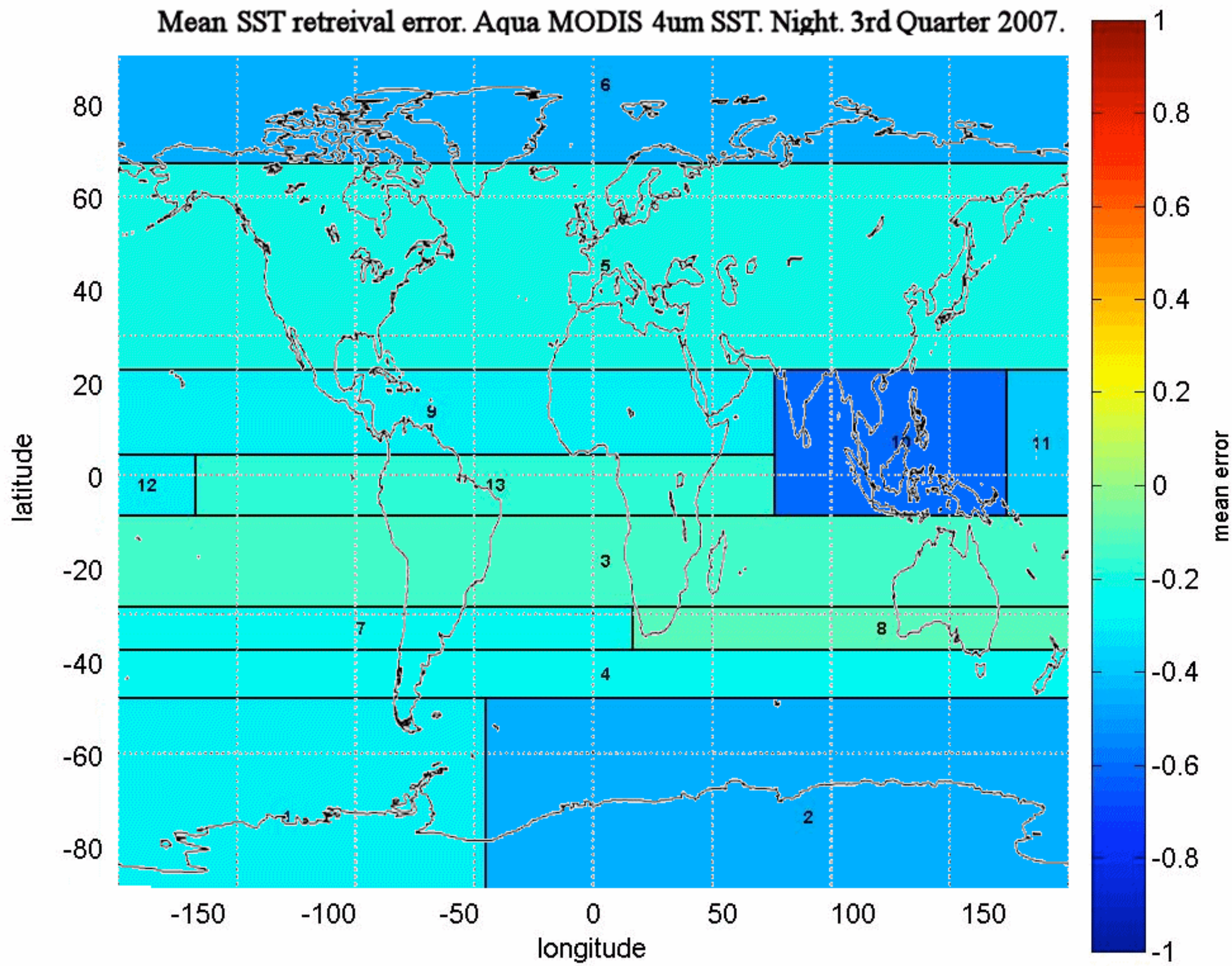

UNIVERSITY OF MIAMI

Std. Dev of SST retreival error. Aqua MODIS 4um SST. Night. 3rd Quarter 2007.

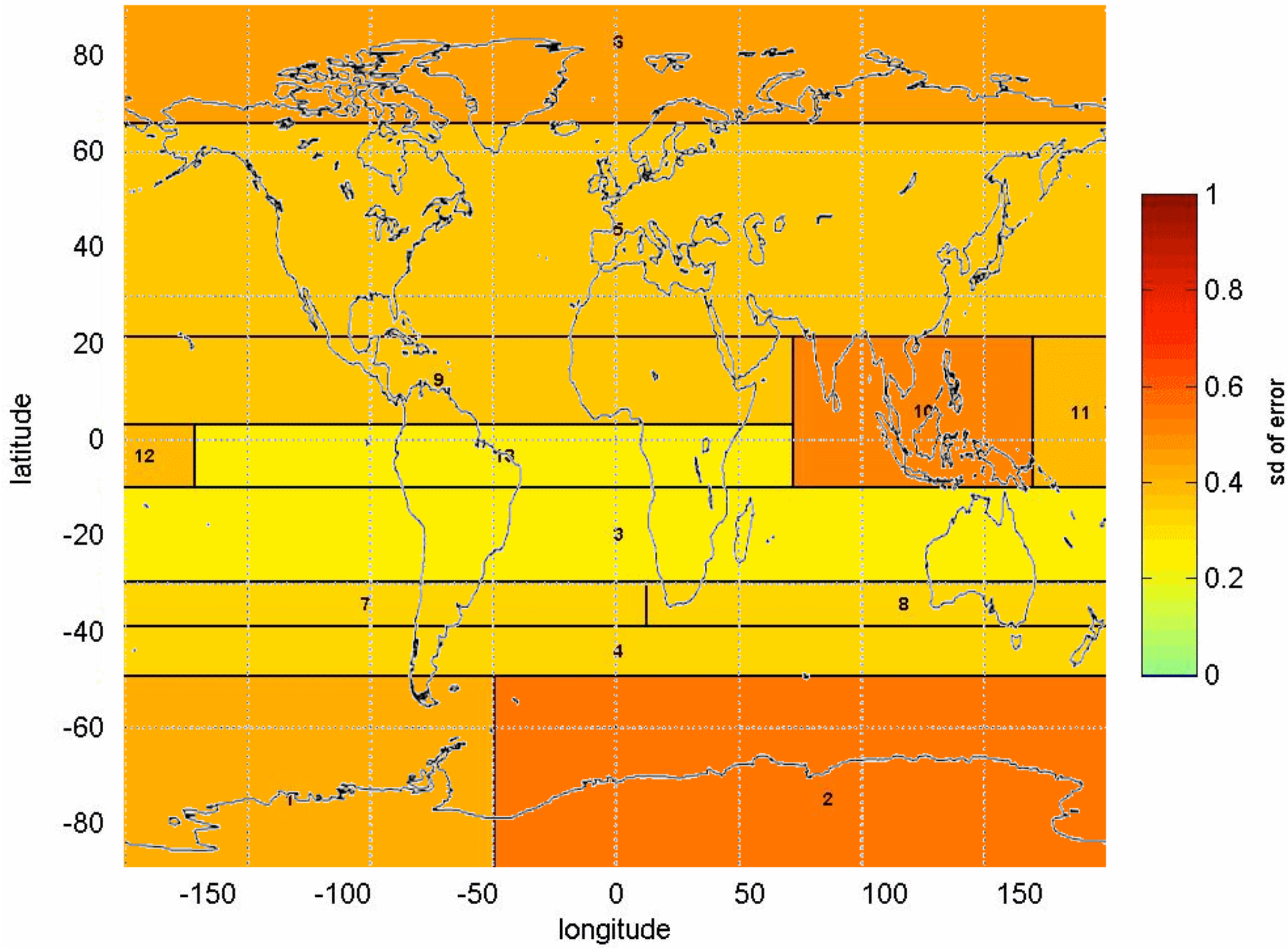

UNIVERSITY OF MIAMI

Regression tree performance

- Terra 2004 SSTday

  NLSST (no regions) – RMSE: 0.581

  New formula (no regions) – RMSE: 0.615

  New formula (with regions) – RMSE: 0.568

- Terra 2004 SST4 (night)

  SST4 (no regions) – RMSE: 0.528

  New formula (no regions) – RMSE: 0.480

  New formula (with regions) – RMSE: 0.456

Support Vector Machines (SVM)

- Best accuracy observed when data set is large (lower accuracy when splitting into regions)
  - Terra 2004 SSTday –
    - RMSE (no region): 0.513, RMSE (with regions): 0.557
- Problems:
  - Computational costs
  - Black-box approach